Universidade de São Paulo–USP
Escola de Engenharia de São Carlos
Departamento de Engenharia Elétrica e de Computação

Aliel Kauchakje Pedrosa

Calculation of the complex permittivity of multi-phase mixtures using the discrete-dipole approximation

São Carlos
2014

Aliel Kauchakje Pedrosa

Calculation of the complex permittivity of multi-phase mixtures using the discrete-dipole approximation

Trabalho de Conclusão de Curso apresentado
à Escola de Engenharia de São Carlos, da
Universidade de São Paulo

Curso de Engenharia Elétrica com ênfase em Eletrônica

ORIENTADOR: Ben-Hur Viana Borges

São Carlos
2014

Kauchakje Pedrosa, Aliel
KK21c Calculation of the complex permittivity of multi-phase mixtures using the discrete-dipole approximation / Aliel Kauchakje Pedrosa; orientador Ben-Hur Viana Borges. São Carlos, 2014.

Monografia (Graduação em Engenharia Elétrica com ênfase em Eletrônica) -- Escola de Engenharia de São Carlos da Universidade de São Paulo, 2014.

1. Electromagnetism. 2. Discrete-dipole approximation. 3. Effective permittivity of mixtures. 4. Dyadic Green's function. 5. Dielectric properties of materials. 6. Mixing rules. I. Título.

FOLHA DE APROVAÇÃO

Nome: Aliel Kauchakje Pedrosa

Título: "Calculation of the complex permittivity of multi-phase mixtures using the discrete-dipole approximation"

Trabalho de Conclusão de Curso defendido e aprovado em 24 / 11 / 2014,

com NOTA 10,0 (DEZ, ZERO), **pela Comissão Julgadora:**

Prof. Associado Ben-Hur Viana Borges - (Orientador - SEL/EESC/USP)

Prof. Dr. João Paulo Pereira do Carmo - (SEL/EESC/USP)

Mestre Leone Veiga Muniz - (Doutorando - SEL/EESC/USP)

Coordenador da CoC-Engenharia Elétrica - EESC/USP:
Prof. Associado Homero Schiabel

Acknowledgements

Foremost, I would like to thank Dr. Bartłomiej Salski for offering me the internship opportunity where this project started. His insightful advices and ideas were essential to make this project happen.

I would also like to thank my advisor Ben-Hur for his help and for providing me with all meanings to make the measurements I wanted to do and for always accepting my very exotic way of working.

I thank my mentors Hildebrando Munhoz, Marcio Gameiro and Kevin Tung for molding the way I think of science and work, for being always kind and helpful whenever I approached them full of doubts and questions.

I am sincerely thankful to my beloved Simone for her personal support and patience at all times. Without her by my side all my journeys would be much more difficult.

I thank also my parents, for being kind and patient even when their son is not around.

And finally, I would like to thank my dear friends Fernando Arruda, Heinz Suadicani, Hudson Pimenta, João Adorno, Lucas Pacheco, Petrônio Crisóstomo for all the discussions we had - about everything(!) - and for making all my study years much funnier and lighter.

For being such a huge and happy part of my life I thank you all!

"Another roof, another proof."
(Paul Erdös)

Resumo

Kauchakje Pedrosa, Aliel **Calculation of the complex permittivity of multi-phase mixtures using the discrete-dipole approximation**. 96 p. Trabalho de Conclusão de Curso – Escola de Engenharia de São Carlos, Universidade de São Paulo, 2014.

Através do estudo das equações de Maxwell e com auxílio de funções de Green nesse trabalho a expressão para a aproximação por dipolos discretos (DDA) foi derivada. Essa expressão foi utilizada para o cálculo da permissividade complexa de misturas. Resultados de medidas em laboratório e presente na literatura, bem como resultados previstos pela fórmula de Maxwell-Garnett, foram comparados com os resultados usando o método DDA. Uma prova da equivalência entre a fórmula de Maxwell-Garnett, no domínio de validade da última, é dada. Mostrou-se, ainda, que o cálculo da permissividade efetiva através do método DDA é mais geral que grande parte das fórmulas de mistura usualmente utilizadas.

Palavras-chave: Permissividade efetiva de misturas, aproximação por dipolos discretos, teoria de meios efetivos, funções de Green.

Abstract

Kauchakje Pedrosa, Aliel **Calculation of the complex permittivity of multiphase mixtures using the discrete-dipole approximation**. 96 p. Final Course Assignment – São Carlos School of Engineering, University of São Paulo, 2014.

Through the study of Maxwell's equations and Green's functions we derive an expression for the discrete-dipole approximation (DDA). This expression is used then to calculate macroscopic (effective) dielectric properties of mixtures. We compare laboratory measurements of the effective permittivity of mixtures with its calculation using the DDA, the well-known Maxwell Garnett mixing rule. A proof is given that those last two are equivalent in the domain of valitity of Maxwell Garnett formula. We show that the DDA is suitable for effective permittivity calculation and it is more general than some of the most used mixing rules.

Keywords: Mixing rules, discrete-dipole approximation, effective medium theory, dielectric property of materials, dyadic Green's function.

List of Figures

List of Tables

Nomenclature

$\bar{\bar{\mathbf{A}}}$	Interaction matrix
$\mathbf{B}$	Magnetic field
$\mathbf{D}$	Electric displacement field
$\mathbf{E}$	Electric field
G	Scalar Green's function
$\bar{\bar{\mathbf{G}}}$	Dyadic Green's function
$\bar{\bar{\mathbf{G}}}_e$	Electric dyadic Green's function
$\bar{\bar{\mathbf{G}}}_m$	Magnetic dyadic Green's function
$\mathbf{H}$	Magnetic field intensity
$\bar{\bar{\mathbf{I}}}$	Unit dyadic
$\bar{\bar{\mathbf{L}}}$	Depolarization dyadic
$\mathbf{M}$	Magnetization vector
$\mathbf{P}$	Polarization density
c	Speed of light
$\mathbf{j}$	Current density in amperes per square meter
$\mathbf{j}_{micro}$	Microscopic current density
k	Wavenumber
$\mathbf{p}$	Dipole moment
q	Charge

$\mathbf{r}$	A point in space
$\mathbf{v}$	Charge speed
χ	Electric susceptibility
δ	Dirac delta
δ_{ij}	Kronecker delta
ϵ_0	Vacuum permittivity
ϵ_r	Relative permittivity
ϵ_{eff}	Effective or equivalent permittivity
μ_0	Vacuum permeability
ω	Angular frequency
ρ	Charge density in coulombs per cubic meter
ρ_f	Free charge density
ρ_{micro}	Microscopic charge density
σ	Electrical conductivity
MG	Maxwell Garnett mixing rule
NRW	Nicolson-Ross-Wier parameter extraction method
∂V	Boundary of a volume V
TRL	trhu-reflect-line VNA calibration
VNA	Vector network analyzer
DDA	Discrete dipole approximation

Contents

Chapter 1

Introduction

The possibility to control macroscopic electrical properties by tuning the microscopic composition of a material plays a central role in modern science. Nanotechnology has been used to the most diverse applications, from finding new inks to try to cure cancer. Wave-material interaction and optical properties of matter also regained the public attention in the last few years. There is also, nowadays, a hype surrounding the synthesis of artificial materials with characteristics that cannot be founded in nature - the so called metamaterials.

The will to control nature and its electric properties is not recent - electrostatics studies date from ancient Greece and surface plasmons have been used for many years to control the color of cathedral windows.

In the beginning of the twentieth century, Maxwell Garnett did a systematic study of color in metallic fields and derived what is yet the most popular mixing rule - a formula to predict a effective parameter based on the microscopic ones.

In modern days similar problems are still relevant. How can we combine materials to perform electromagnetic shielding? How can we mix materials so we can control the losses inside a optical fiber or an optical modulator? How much graphene would be necessary to put inside a dielectric ink to make it conductive?

Motivated by this questions and by the limitations of the most used mixing formulas a different approach for calculating the effective permittivity of a mixture is proposed. The method relies on the discrete-dipole approximation (DDA), a well-known technique used to calculate scattering properties of materials. The main advantage of using this method is that for any geometric distribution of inclusions inside a host and for any number of phases, the procedure is the same.

This document will be composed by six chapters that may be read independently.

The second chapter is a reminder of how Maxwell's equations may be written in a material media. It introduces essential concepts and the most basic set of equations that will be used for more complex formulations.

The third chapter is a reminder on electrostatics in order to clarify the differences

between the local and macroscopic field and give intuition on the depolarization field.

The fourth chapter is the true basis of the DDA formulation. Using a dyadic Green's function the total electric field for a scatterer is rigorously calculated. The mathematical development of the equations make some important concepts to appear naturally - it is the case for the depolarization tensor, for example. Having intuition on the whole derivation process is also important to have a better understanding and intuition on the mechanics of the DDA.

The following chapter presents briefly the DDA as it is used and, in the subsequent chapter will state the mixing problem and use the DDA formulation to solve it. A comparison will be made between the Maxwell Garnett formula and the proposed method.

In order to verify the validity of the proposed method, calculations are compared with experiments and with results gathered in the literature.

Chapter 2

Maxwell's macroscopic equations and constitutive relations

We start by recalling Maxwell's equations and presenting the problem of calculating macroscopic quantities.

Macroscopic quantities are spatially filtered quantities. All microscopic changes must be ignored.

We shall formalize this filtering idea and present a set of equations that are known by Maxwell's equation in matter.

The final section of this chapter will present some important constitutive relations that will be used exhaustively during this dissertation.

2.1 Maxwell's equations in vacuum

We remember the equations describing the spatial and temporal evolution of the electric and magnetic fields in the vacuum.

$$\begin{aligned} \nabla \cdot \mathbf{B} &= 0 \\ \nabla \cdot \mathbf{E} &= \frac{\rho}{\epsilon_0} \\ \nabla \times \mathbf{B} &= \mu_0 \mathbf{j} + \epsilon_0 \mu_0 \frac{\partial \mathbf{E}}{\partial t} \\ \nabla \times \mathbf{E} &= -\frac{\partial \mathbf{B}}{\partial t} \end{aligned} \tag{1}$$

The set of equations (1) is called Maxwell's equations and here they are written in SI units (JACKSON, 1999).

Another remarkable relation is given by 2 and defines the speed of light in the vacuum.

$$c = \frac{1}{\sqrt{\epsilon_0 \mu_0}} \tag{2}$$

2.2 Maxwell's equations in matter

When we consider an electromagnetic wave propagating in the vacuum we suppose that the source is far from the test particle and that this particle is isolated. When the wave is propagating in a material medium the test particle is surrounded by other source points - electrons and nuclei of the atoms that constitutes the material. If we consider that we may have around 10^{23} particles per unit volume, the calculation of electromagnetic fields using equations (1) and (3), that takes into account each and every microscopic particle, is neither convenient nor practical.

$$\begin{aligned} \rho_{micro}(\mathbf{r},t) &= \sum_i q_i \delta[\mathbf{r}-\mathbf{r}_i(t)] \\ \mathbf{j}_{micro}(\mathbf{r},t) &= \sum_i q_i \mathbf{v}_i(t)\delta[\mathbf{r}-\mathbf{r}_i(t)] \end{aligned} \tag{3}$$

Where $\mathbf{r}$ is a point in the space and $\mathbf{r}_i$, q_i and $\mathbf{v}_i$ are the position, the charge and the speed of a charge i.

For macroscopic observations we are not interested in the variations coming from the interaction between those small sources. The relevant quantity are averaged fields that we will call from now on macroscopic fields (MARQUIER, 2012).

2.2.1 Spatial averages

In order to establish a new set of equations describing the averaged behavior of electromagnetic fields in a material medium we need to define a spatial average and study its properties.

Two goals are achieved using averaged fields:

- ❑ All fast variations in ρ, $\mathbf{j}$, $\mathbf{E}$ and $\mathbf{B}$ are eliminated.
- ❑ ρ_{micro} and $\mathbf{j}_{micro}$ are mathematical distributions with δ-type singularities. Averaging will replace this distribution by continuous functions.

We consider a function $f(\mathbf{r})$ with a compact support of typical length L_0. This typical length should be much bigger than the size of one atom, but small if compared to the wavelength. We want this function to verify (4) for it to be a probability density function.

$$\int f(\mathbf{r}) d^3\mathbf{r} = 1 \tag{4}$$

By definition, the averaged charge density is given by (5).

$$\langle \rho_{micro} \rangle(\mathbf{r}) = \int \rho_{micro}(\mathbf{r}') f(\mathbf{r}-\mathbf{r}') d^3\mathbf{r}' \tag{5}$$

For the sake of clarity one example is given.

2.2.1.1 Case of a single particle

Suppose a single charge q in a position $\mathbf{r}_0(t)$. From (3):

$$\rho_{micro} = q\delta[\mathbf{r} - \mathbf{r}_0(t)] \tag{6}$$

Applying the averaging function, from (5):

$$\langle\rho_{micro}\rangle(\mathbf{r}) = \int \rho_{micro}(\mathbf{r})' f(\mathbf{r} - \mathbf{r}')d^3\mathbf{r}' = qf(\mathbf{r} - \mathbf{r}_0(t)) \tag{7}$$

We can see by mean of equation (7) that the charge is continuously distributed in a typical volume L_0^3 instead of being a singularity.

2.2.1.2 Deriving an averaged function

Since the averaging function f has a compact support we can show that the average of the derivative is the derivative of the average.

$$\langle\partial_i A\rangle = \partial_i\langle A\rangle \tag{8}$$

This result is intuitive if we understand the averaging function as a linear low-pass filter for spatial frequencies and knowing that the derivative is a linear operator.

2.2.2 Macroscopic Gauss's law

Let's start calculating the macroscopic Maxwell equations by averaging the Gauss law. From (1), being $\mathbf{E}_{micro}$ the electric field accounting for all microscopic effects we want to average:

$$\begin{aligned} \nabla \cdot E_{micro} &= \frac{\rho_{micro}}{\epsilon_0} \\ \langle\nabla \cdot E_{micro}\rangle &= \frac{\langle\rho_{micro}\rangle}{\epsilon_0} \\ \nabla \cdot \langle E_{micro}\rangle &= \frac{\langle\rho_{micro}\rangle}{\epsilon_0} \end{aligned} \tag{9}$$

In order to have an expression for $\nabla \cdot \langle E_{micro}\rangle$ we need to have an expression for $\langle\rho_{micro}\rangle$.

2.2.2.1 Calculation of $\langle\rho_{micro}\rangle$

In this section we will call atoms every group of bounded charges: it may be an ion, or a molecule, for example. Atom is then the smallest element analyzed and may differ from the definition of a physical atom. This nomenclature is, however, widely used in the literature.

We consider here the case of an isolated composed by particles with position $\mathbf{r}_i$. Let's also consider that the coordinate system is centered at the center of mass of that atom. The charge density of this atom is given by equation (10)

$$\rho_{at}(\mathbf{r}) = \sum_i q_i \delta[\mathbf{r} - \mathbf{r}_i] \tag{10}$$

Averaging it we get:

$$\langle \rho_{at}(\mathbf{r}) \rangle = \sum_i q_i f(\mathbf{r} - \mathbf{r}_i) \tag{11}$$

We assume that all the particles are close to each other in an atomic scale. The choice of f is such that it has very small variations in that atomic scale, we can than expand (11) in a first order Taylor expansion.

$$\langle \rho_{at}(\mathbf{r}) \rangle = \sum_i q_i f(\mathbf{r}) - \sum_i q_i \mathbf{r}_i \cdot \nabla f(\mathbf{r}) = f(\mathbf{r}) \sum_i q_i - \left(\sum_i q_i \mathbf{r}_i \right) \cdot \nabla f(\mathbf{r}) \tag{12}$$

The sum $(\sum_i q_i)$ in (12) is the total charge of the atom and it is denoted by q. The sum $(\sum_i q_i \mathbf{r}_i)$ is called dipole moment of the atom. The dipole moment is denoted by $\mathbf{p}$ and it is a gauge of the overall polarity of the atom.

$$\mathbf{p}_{at} = \sum_i q_i \mathbf{r}_i \tag{13}$$

The understanding of this quantity is crucial for the development of the following chapters since, as we shall see, it is the quantity that the DDA method will help us calculate.

It is important to note that even a neutral atom may have a non-null average charge density since the atom may be polarized by an external field or it may have a permanent dipole moment.

If we now consider not only one single atom but the set of atoms that composes the material the average charge density is the contribution of all atoms.

In order to recenter our coordinate system we denote the center of mass of each atom as $\mathbf{r}_a$, so everywhere we had $f(\mathbf{r})$ is now $f(\mathbf{r} - \mathbf{r}_a)$.

Also using the index a to denote each atom and ρ to denote the total charge density, we have:

$$\begin{aligned} \langle \rho(\mathbf{r}) \rangle &= \langle \sum_a \rho_a(\mathbf{r}) \rangle \\ &= \sum_a \langle \rho_a(\mathbf{r}) \rangle \\ &= \sum_a q_a f(\mathbf{r} - \mathbf{r}_a) - \sum_a \mathbf{p}_a \cdot \nabla f(\mathbf{r} - \mathbf{r}_a) \end{aligned} \tag{14}$$

We recall the following vector identity:

$$\mathbf{p}_a \cdot \nabla f(\mathbf{r} - \mathbf{r}_a) = \nabla \cdot (\mathbf{p}_a f(\mathbf{r} - \mathbf{r}_a)) - f(\mathbf{r} - \mathbf{r}_a) \nabla \cdot \mathbf{p}_a \tag{15}$$

We consider that $\mathbf{p}_a$ is a constant vector and then $\nabla \cdot \mathbf{p}_a = 0$. Equation (15) becomes:

$$\mathbf{p}_a \cdot \nabla f(\mathbf{r} - \mathbf{r}_a) = \nabla \cdot (\mathbf{p}_a f(\mathbf{r} - \mathbf{r}_a)) \tag{16}$$

The total charge density may be then written as:

$$\langle \rho(\mathbf{r}) \rangle = \sum_a q_a f(\mathbf{r} - \mathbf{r}_a) - \nabla \cdot \sum_a (\mathbf{p}_a f(\mathbf{r} - \mathbf{r}_a)) \tag{17}$$

We define then another important quantity, the polarization or polarization density:

$$\mathbf{P}(\mathbf{r}) = \sum_a \mathbf{p}_a f(\mathbf{r} - \mathbf{r}_a) \tag{18}$$

The first term on the right hand side of equation (17) is called free charge density and it will be denoted by ρ_f. Combining this new notation, equation (18) and (9), we have:

$$\nabla \langle E_{micro} \rangle = \frac{\rho_f - \nabla \cdot \mathbf{P}}{\epsilon_0} \tag{19}$$

We introduce the electric displacement field (20):

$$\mathbf{D} = \epsilon_0 \mathbf{E} + \mathbf{P} \tag{20}$$

Hereafter the brackets for averaged fields will be omitted since every relevant quantity is averaged. Using equation (20) Gauss's law assumes a simple and condensed form:

$$\nabla \cdot \mathbf{D} = \rho_f \tag{21}$$

2.2.3 Macroscopic Ampère's law

In a similar way we can calculate $\langle \mathbf{j}_{micro} \rangle$ and introducing the magnetization vector $\mathbf{M}$ and magnetic field $\mathbf{H}$ we will reach:

$$\nabla \times \mathbf{H} = \mathbf{j}_f + \partial_t \mathbf{D} \tag{22}$$

with

$$\mathbf{H} = \frac{\mathbf{B}}{\mu_0} - \mathbf{M} \tag{23}$$

2.2.4 Conclusions

The other two equations may be written as:

$$\begin{aligned} \nabla \times \langle \mathbf{E} \rangle &= -\partial_t \langle \mathbf{B} \rangle \\ \nabla \times \langle \mathbf{B} \rangle &= 0 \end{aligned} \tag{24}$$

Equations 20, 21, 23 and 22 show that in order to find the unknown fields $\mathbf{D}$ and $\mathbf{H}$ we need to know the function linking $\mathbf{P}$ and $\mathbf{E}$, $\mathbf{D}$ and $\mathbf{E}$ and $\mathbf{B}$ and $\mathbf{H}$.

The equations making those links are called constitutive relations and they depend on the material we are considering.

The equations presented in this section, together with the constitutive relations will allow us to extend the microscopic Maxwell's equations to the macroscopic ones.

2.3 Constitutive relations

Constitutive relations are equations linking any two physical quantities. The former section showed the need to establish relations between **D**, **E**, **P**, **B** and **H** in order to have Maxwell's equations reformulated.

2.3.1 Ohm's law

The well known Ohm's law may can be written in terms of **j** and **E** by:

$$\mathbf{j} = \sigma \mathbf{E} \tag{25}$$

where σ is the electrical conductivity.

As expected, an insulating material such as rubber has a conductivity of order 10^{-13}S/m, with means that even with a really strong electric field almost no current will flow.

2.3.2 Polarization density and electric field

The polarization density **P** is related to **E** in a very general way by the series expansion given by equation (26):

$$P_i = \epsilon_0(\chi_{ij}E_j + \chi_{ijk}E_jE_k + ...) \tag{26}$$

The quantity χ is called electric susceptibility of the medium.

If the electric field is smaller than the inter-atomic electric fields, around 10^8V/m, the non-linear terms of equation (26) may be neglected and it becomes:

$$\mathbf{P} = \epsilon_0 \chi \mathbf{E} \tag{27}$$

Although simpler than equation (26), χ in equation (27) is a second order tensor once the medium may be anisotropic.

2.3.3 Locality and dispersion

When writing equations 25 and 27 we have omitted, for sake of clarity, the dependencies of **j** , σ, χ, **P** and **E** with the space and frequency, i.e., $a = a(\omega, \mathbf{r})$.

Locality implies that the movement of one electron is only dependent of the electric field exactly in the point where this electron is found. If the wavelength is much greater than one electron's mean free path we can assume locality. This will be considered true if not stated otherwise.

The relation of the physical quantities with the frequency is called dispersion and since it is related to the response time of a material will it can be neglected in semi-static or static approximations. That will not be the case and unless otherwise stated we will always consider dispersive media.

2.3.4 Relative permittivity

The relative permittivity or dielectric constant ϵ_r is the quantity that yields $\mathbf{D}$ and $\mathbf{E}$ via:

$$\mathbf{D} = \epsilon_0 \epsilon_r \mathbf{E} \tag{28}$$

Through equation (27) we may see that ϵ_r is a second order tensor and it is related to the electrical susceptibility by:

$$\chi = \epsilon_r - \mathbf{I} \tag{29}$$

where $\mathbf{I}$ is the unit second order tensor.

2.3.5 Magnetic permeability

The magnetic permeability μ_r is the physical quantity linking $\mathbf{B}$ and $\mathbf{H}$ for a magnetic material.

$$\mathbf{B} = \mu_0 \mu_r \mathbf{H} \tag{30}$$

Unless otherwise stated, from now on μ_r will be considered unitary and the magnetization $\mathbf{M}$ is considered zero.

2.3.6 Static and dynamic fields

When the electromagnetic field is not varying in time, e.g. when a battery is the voltage source to a lamp, $\partial_t \mathbf{P} = 0$ and the only contribution to the electric current is $\mathbf{j}_f$. In this case the material can be characterized by a resistance measurement that will give the conductivity $\sigma(\omega = 0)$ and by a capacitance measurement that will give the permittivity $\epsilon_r(\omega = 0)$.

If, however, $\partial_t \mathbf{P} \neq 0$ the effects of bounded and free charges are combined and it is not possible to define conductivity and permittivity as before. For a monochromatic excitation we define then an effective electric current density as

$$\begin{aligned} \mathbf{j}_{eff}(\mathbf{r}, \omega) &= \sigma(\omega)\mathbf{E}(\mathbf{r}, \omega) - i\omega \mathbf{P}(\mathbf{r}, \omega) \\ &= [\sigma(\omega) - i\omega\epsilon_0(\epsilon_r(\omega) - 1)]\mathbf{E}(\mathbf{r}, \omega) \end{aligned} \tag{31}$$

The term between square brackets in (31) is called complex conductivity. Hence:

$$\sigma_{eq} = \sigma(\omega) - i\omega\epsilon_0(\epsilon_r(\omega) - 1) \tag{32}$$

Since $\mathbf{j} = -i\omega\mathbf{P}$ we define one equivalent polarization density $\mathbf{P}_{eff}$ as:

$$\mathbf{P}_{eff} = \epsilon_0(\epsilon_{eff} - 1)\mathbf{E} \tag{33}$$

with

$$\epsilon_{eff} = \epsilon_r + i\frac{\sigma}{\omega\epsilon_0} \tag{34}$$

We will assume hereafter that all quantities will be the equivalent or effective ones here calculated and the subscript 'eff' will be omitted.

2.4 Conclusions

Using the results presented on the two former sections we can rewrite Maxwell's equation in a much more convenient form for calculations in a material medium.

Equation (22) becomes:

$$\nabla \times \mathbf{H} = \partial_t \mathbf{D} \tag{35}$$

with

$$D = D_{eff} = \epsilon_0 \epsilon_{eff} \mathbf{E} \tag{36}$$

Using the charge conservation principle $\nabla \cdot \mathbf{j}_f = i\omega\rho_f$, equation (21) becomes:

$$\nabla \cdot D = \nabla \cdot D_{eff} = 0 \tag{37}$$

The new set of Maxwell's can be written then as:

$$\begin{aligned} \nabla \cdot \mathbf{B} &= 0 \\ \nabla \cdot \mathbf{D} &= 0 \\ \nabla \times \mathbf{H} &= \partial_t \mathbf{D} \\ \nabla \times \mathbf{E} &= -\partial_t \mathbf{B} \end{aligned} \tag{38}$$

Chapter 3

Macroscopic versus local field

Chapter 2 presents averaged quantities in order to 'filter' any rapid variation of the electric and magnetic field inside a dielectric. These quantities are called macroscopic fields. If we are, however, interested in a smaller scale we cannot make use of the spatial average used before.

The local field, the one that acts at a given point in the space, is strongly influenced by the surroundings of the test point and it is usually different form the macroscopic field.

In this chapter we shall clarify the difference between the macroscopic and the local electric fields and point out their relation with dielectric properties of materials.

Hereafter, unless otherwise stated, the index *loc* will be used to represent local fields, the index *inc* to represent the incident field, *dep* to represent the depolarization field and the macroscopic field will be used without any index.

The electric fields are assumed here to be uniform. In all other chapters this assumption is not true. However, if we consider that the wavelength of the electric field is much greater (quasi-static or static approximation) than the size of the dielectric body in study, all the results derived here are true.

3.1 Depolarization field

When a dielectric body is illuminated by an electric field $\mathbf{E}_{inc}$ it will polarize and this polarization will generate a electric field $\mathbf{E}_{dep}$ inside this body. This electric field opposes the incident electric field and, for that, it is called depolarization field.

The calculation of the depolarization field due to an uniform polarization $\mathbf{P}$ is calculated using the electrostatic potential (JACKSON, 1999). For simple geometries such as ellipsoids, one can prove that a uniform polarization creates a uniform depolarization field and those two quantities are proportional. The proportionality factor is called depolarization tensor, or depolarization factor, and it will be appear naturally on the development of the expression for the total field in Chapter 4.

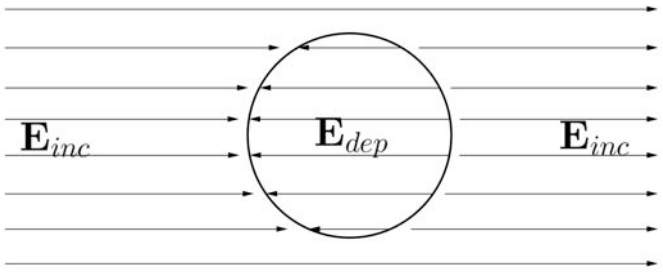

Figure 1: Dielecric sphere in a uniform field E_{inc} with opposing field created by its polarization.

3.1.1 The case of a sphere

The main interest of this chapter, besides given an intuition on the differences between the macroscopic and local field, is to make a link between all relevant physical quantities to the dielectric properties of a given dielectric body.

In order to show how those links are made, the example of a dielectric sphere of permittivity ϵ_r will be given. For a dielectric sphere, the expression for the depolarization field is given by (JACKSON, 1999):

$$\mathbf{E}_{dep} = -\frac{1}{3\epsilon_0}\mathbf{P} \tag{39}$$

The macroscopic field, i.e., the average field sensed by this sphere, is calculated simply by:

$$\mathbf{E} = \mathbf{E}_{inc} + \mathbf{E}_{dep} = \mathbf{E}_{inc} - \frac{1}{3\epsilon_0}\mathbf{P} \tag{40}$$

Using equation (33):

$$\begin{aligned} \mathbf{P} &= \epsilon_0\chi\mathbf{E} \\ &= \epsilon_0\chi\left(\mathbf{E}_{inc} - \frac{1}{3\epsilon_0}\mathbf{P}\right) \end{aligned} \tag{41}$$

Hence:

$$\epsilon_{r_j} = 1 + \frac{P_j}{\epsilon_0 E_{inc_j} - \frac{1}{3}P_j} \tag{42}$$

Equation (42) shows that knowing the polarization density $\mathbf{P}$ is sufficient to know the relative permittivity of a dielectric sphere.

3.2 Local field

The local field at a dipole is the total electric field acting on this dipole. This field is a superposition of the incident electric field, the depolarization field and the interaction of the test dipole and all other surrounding dipoles.

The local field is then a microscopic quantity and it is extremely dependent on the position were it is measured.

3.2.1 The case of a sphere in a cubic lattice

If we consider a collection of spherical dipoles in a cubic lattice we can prove that the local field, due to the symmetry of the problem, is equal to the incident electric field (TSYMBAL, 2013). We can then write it in terms of the macroscopic electric using equation (40).

$$\mathbf{E}_{loc} = \mathbf{E}_{inc} = \mathbf{E} + \frac{1}{3\epsilon_0}\mathbf{P} \tag{43}$$

The local field is then greater than the macroscopic field by a factor that depends of the polarization of the dielectric sphere.

We remember that our ultimate goal is to relate all those quantities with the permittivity of the sphere and then, in order to link the polarization with the local field, we introduce the notion of polarizability. The polarizability (α) is the physical quantity that gauges how much the dipole moment of a dipole changes with its exciting electric field. In our case, this exciting electric field is the local field and the polarizability is calculated by:

$$\mathbf{p} = \alpha\mathbf{E}_{loc} = \alpha\mathbf{E}_{inc} \tag{44}$$

Since the polarization density is the density of dipole moments it can be written by:

$$\begin{aligned} \mathbf{P} &= \sum_i N_i \mathbf{p}_i \\ &= \left(\sum_i N_i \alpha_i\right) \mathbf{E}_{inc} \end{aligned} \tag{45}$$

where N_i is the number of dipoles of type i per unit volume.

Using equation (42) we reach:

$$\epsilon_{r_j} = 1 + \frac{\sum_i N_i\alpha_i}{\epsilon_0 - \frac{1}{3}\sum_i N_i\alpha_i} \tag{46}$$

This equation is called the Clausius-Mossotti equation and it is best know in the following equivalent formulation:

$$\frac{\epsilon - \epsilon_0}{\epsilon + 2\epsilon_0} = \frac{1}{3\epsilon_0}\sum_i N_i\alpha_i \tag{47}$$

where $\epsilon = \epsilon_0\epsilon_r$.

3.3 Remarks and conclusion

In this chapter the differences between the local and macroscopic field were presented. Through an overview of the case of a dielectric sphere we could derive important results linking those quantities and the dielectric properties of that sphere.

The concepts presented here are the base for the derivations made on the next chapters and are a essential key to understand and solving the mixing problem.

Chapter 4

Free space dyadic Green's function

In this chapter we are interested in calculating the total electric field inside a dielectric scatterer in free space. This scatterer is illuminated by an electric field $\mathbf{E}_{inc}$, it is supposed to be non-magnetic and it has a volume V. Here $F \setminus V$ is used to denote everywhere but V. Hence $F = F \setminus V \cup V$ is the whole free space.

From Maxwell's curl equations (1):

$$\begin{aligned} \nabla \times \mathbf{E}(\mathbf{r}) - i\omega \mathbf{B}(\mathbf{r}) &= 0 \\ \nabla \times \mathbf{B}(\mathbf{r}) + i\omega\epsilon_0\mu_0\mathbf{E} &= \mu_0 \mathbf{j}(\mathbf{r}), \quad \mathbf{r} \in F \end{aligned} \tag{48}$$

Using previous results, the source term in (48) can be calculated by:

$$\begin{aligned} \mathbf{j}(\mathbf{r}) &= 0, \quad \mathbf{r} \in F \setminus V \\ \mathbf{j}(\mathbf{r}) &= -i\omega\epsilon_0(\epsilon_r(\mathbf{r}) - \mathbf{I})\mathbf{E}, \quad \mathbf{r} \in V \end{aligned} \tag{49}$$

The solution for the electric field equation in (48) is given by the integral equation (LAKHTAKIA, 1992) (50):

$$\begin{aligned} \mathbf{E}(\mathbf{r}) - \mathbf{E}_{inc}(\mathbf{r}) &= \int_{V_0} d^3r' (i\omega\mu_0 \bar{\bar{\mathbf{G}}}(\mathbf{r}, \mathbf{r}')\mathbf{j}(\mathbf{r}')) \\ &= \int_{V_0} d^3r' (k_0^2 \bar{\bar{\mathbf{G}}}(\mathbf{r}, \mathbf{r}')\mathbf{E}(\mathbf{r}')), \quad \mathbf{r} \in F \end{aligned} \tag{50}$$

The dyadic $\bar{\bar{\mathbf{G}}}$ is the free space dyadic Green's function. In this chapter we shall find an expression for $\bar{\bar{\mathbf{G}}}$ and develop (50) in a way to avoid the singularities that may arise.

4.1 Free space Green's function

Before calculating the dyadic Green's function for free space we calculate the Green's function for the inhomogeneous wave equation (51).

$$(\nabla^2 - k_0^2 \partial_t^2) f = -\frac{\rho(\mathbf{r}, t)}{\epsilon_0} \tag{51}$$

Writing the same equation for the Green's function and taking the Fourier transform in relation to $\mathbf{r}$ and t:

$$(-k^2 + k_0^2)G(\mathbf{k}, \omega) = -1 \tag{52}$$

Since G is a distribution (in the mathematical sense), the result of equation (52) is given by:

$$G(\mathbf{k}, \omega) = pv\left(\frac{1}{k^2 - k_0^2}\right) + C\delta(k - k_0) + C'\delta(k + k_0) \tag{53}$$

where pv represents the principal value of a distribution and C and C' are constants defined by the boundary conditions.

Applying the inverse Fourier transform in respect to $\mathbf{k}$ on (53) we reach:

$$G(\mathbf{r}, \omega) = pv \int \frac{1}{(2\pi)^3} G(\mathbf{k}, \omega) \exp(i\mathbf{k} \cdot \mathbf{r}) d^3\mathbf{k} \tag{54}$$

Rewriting (54) in a spherical coordinate system it is easy to see that $G(\mathbf{r}, \omega)$ is:

$$\begin{aligned} G(\mathbf{r}, \omega) &= \frac{1}{2\pi^2 r} Im\left[pv \int_0^\infty kG(\mathbf{k}, \omega) \exp(ikr) dk\right] \\ &= \frac{1}{2\pi^2 r} Im\left[pv \int_0^\infty \left(\frac{k}{k^2 - k_0^2} + Ck\delta(k - k_0) + C'k\delta(k + k_0)\right) \exp(ikr) dk\right] \\ &= \frac{1}{4\pi r}\left(Res(k_0) + Res(-k_0)\right) + \frac{1}{2\pi^2 r} Im\left[Ck_0 \exp(ik_0 r)\right] + 0 \\ &= \frac{1}{4\pi r} \cos(k_0 r) + \frac{1}{2\pi^2 r} Ck_0 \sin(ik_0 r) \end{aligned} \tag{55}$$

Equation (55) may be written in function of complex exponential functions so the physical meaning of waves coming to and from the source are easily identified. Introducing two dummy constants K and K'.

$$G(\mathbf{r}, \omega) = K\frac{\exp(ik_0 r)}{r} + K'\frac{\exp(-ik_0 r)}{r} \tag{56}$$

Sommerfeld radiation condition implies that should be no energy sinking at the source, so K' must be zero.

$$\begin{aligned} K' &= \frac{1}{4\pi} + \frac{iCk_0}{2\pi^2} \\ &= 0 \end{aligned} \tag{57}$$

We can then calculate $C = i\pi(2k_0)^{-1}$ and hence

$$G(\mathbf{r}, \omega) = \frac{1}{4\pi r} \exp(ik_0 r) \tag{58}$$

4.2 Dyadic Green's function

When finding the scalar Green's function (58) the source was supposed to be scalar. If we consider a vector source $\mathbf{j}(\mathbf{r})$, by using both equations in (48):

$$\begin{aligned} \nabla \times \nabla \times \mathbf{E} &= i\omega \mathbf{B} \\ &= k_0^2 \mathbf{E} + i\omega\mu_0 \mathbf{j} \end{aligned} \tag{59}$$

Isolating the source on the right hand side of (59) the Green's function to be found must be the result of the differential equation (60):

$$\begin{aligned} ((\nabla \times \nabla \times) - k_0^2)\bar{\bar{\mathbf{G}}}(\mathbf{r}, \mathbf{r}') &= \\ ((\nabla\nabla\cdot) - \nabla^2 - k_0^2)\bar{\bar{\mathbf{G}}}(\mathbf{r}, \mathbf{r}') &= \bar{\bar{\mathbf{I}}}\delta[\mathbf{r} - \mathbf{r}'] \end{aligned} \tag{60}$$

In order to find $\nabla\nabla \cdot \bar{\bar{\mathbf{G}}}$ we take the divergence of (60).

$$\begin{aligned} \nabla \cdot ((\nabla \times \nabla \times) - k_0^2)\bar{\bar{\mathbf{G}}}(\mathbf{r}, \mathbf{r}') &= \nabla \cdot (\bar{\bar{\mathbf{I}}}\delta[\mathbf{r} - \mathbf{r}']) \\ &= (\nabla \cdot \bar{\bar{\mathbf{I}}})\delta + \bar{\bar{\mathbf{I}}}\nabla\delta \\ &= \nabla\delta \end{aligned} \tag{61}$$

Since $(\nabla \cdot \nabla \times \mathbf{A}) = 0$:

$$-k_0^2 \nabla \cdot \bar{\bar{\mathbf{G}}}(\mathbf{r}, \mathbf{r}') = \nabla\delta \tag{62}$$

Taking the gradient of equation (62).

$$-k_0^2 \nabla\nabla \cdot \bar{\bar{\mathbf{G}}}(\mathbf{r}, \mathbf{r}') = \nabla\nabla\delta \tag{63}$$

Hence

$$\nabla\nabla \cdot \bar{\bar{\mathbf{G}}}(\mathbf{r}, \mathbf{r}') = -\frac{1}{k^2}\nabla\nabla\delta[\mathbf{r} - \mathbf{r}'] \tag{64}$$

and the equation (60) becomes:

$$(\nabla^2 + k_0^2)\bar{\bar{\mathbf{G}}}(\mathbf{r}, \mathbf{r}') = -\left(\bar{\bar{\mathbf{I}}} + \frac{\nabla\nabla}{k^2}\right)\delta[\mathbf{r} - \mathbf{r}'] \tag{65}$$

One may observe that we can leverage the scalar function G found in Section 4.1, equation (58), since $(\nabla^2 + k^2)G = \delta$. Considering this fact we test $-\left(\bar{\bar{\mathbf{I}}} + \frac{\nabla\nabla}{k^2}\right)G$ as a solution for (60).

$$\begin{aligned} (\nabla^2 + k_0^2) - \left(\bar{\bar{\mathbf{I}}} + \frac{\nabla\nabla}{k^2}\right)G(\mathbf{r}, \mathbf{r}') &= -\left(\bar{\bar{\mathbf{I}}} + \frac{\nabla\nabla}{k^2}\right)(\nabla^2 + k_0^2)G(\mathbf{r}, \mathbf{r}') \\ &\quad - \left(\bar{\bar{\mathbf{I}}} + \frac{\nabla\nabla}{k^2}\right)\delta[\mathbf{r} - \mathbf{r}'] \end{aligned} \tag{66}$$

Using Sommerfeld radiation condition this solution is proven to be unique.

$$\bar{\bar{\mathbf{G}}}(\mathbf{r}, \mathbf{r}') = -\left(\bar{\bar{\mathbf{I}}} + \frac{\nabla\nabla}{k^2}\right)G(\mathbf{r}, \mathbf{r}') \tag{67}$$

We note that since $\bar{\bar{\mathbf{G}}} \propto G$, the dyadic Green's function has a singularity when $\mathbf{r}$ is equal to $\mathbf{r}'$.

4.3 Removing the singularity

To evaluate the integral in (50) we should remove the singularity introduced by $\bar{\bar{\mathbf{G}}}$. Many techniques may be applied to solve this problem. As shown by Yaghjian (YAGHJIAN, 1980), some developments, although concise and reaching the right result, are not rigorous and should be avoided. Yurkin in (YURKIN; HOEKSTRA, 2007a) emphasizes that different approaches may lead to different results.

We choose to remove the singularity using an approach that is a combination between Yaghjian's (YAGHJIAN, 1980) and Lakhtakia's (LAKHTAKIA, 1992) approaches. Some important concepts will arise on this development, such as the depolarization factor.

The first stage of the development of expression (50) must be understood in depth since it will provide the basic idea on how we will treat the mixing problems - in other words the problem of having inclusions inside a volume.

This insightful and intuitive approach will have as result the equation that will be the basis of the discrete dipole approximation.

4.3.1 Yet another formulation for Maxwell's equations

In order to ease the mathematical burden we shall rewrite the wave equation for the electric field (59) in a more convenient way.

We recall the vector identity:

$$\nabla \times \nabla \times \mathbf{A} = \nabla(\nabla \cdot \mathbf{A}) - \nabla^2 \mathbf{A} \tag{68}$$

We use this identity to calculate $\nabla \times \nabla \times (\mathbf{E} - \frac{\mathbf{j}}{i\omega\epsilon_0})$:

$$\nabla \times \nabla \times \left(\mathbf{E} - \frac{\mathbf{j}}{i\omega\epsilon_0}\right) = \nabla\left(\nabla \cdot \left(\mathbf{E} - \frac{\mathbf{j}}{i\omega\epsilon_0}\right)\right) - \nabla^2\left(\mathbf{E} - \frac{\mathbf{j}}{i\omega\epsilon_0}\right) \tag{69}$$

By Gauss's law and charge conservation equations:

$$\begin{cases} \nabla \cdot \mathbf{E} = \frac{\rho}{\epsilon_0} \\ \nabla \cdot \mathbf{j} - i\omega\rho = 0 \end{cases} \quad \Rightarrow \nabla \cdot \left(\mathbf{E} - \frac{\mathbf{j}}{i\omega\epsilon_0}\right) = 0 \tag{70}$$

Equation (69) then becomes:

$$\nabla \times \nabla \times \left(\mathbf{E} - \frac{\mathbf{j}}{i\omega\epsilon_0}\right) = -\nabla^2\left(\mathbf{E} - \frac{\mathbf{j}}{i\omega\epsilon_0}\right) \tag{71}$$

Subtracting $\nabla \times \nabla \times (\frac{\mathbf{j}}{i\omega\epsilon_0})$ from both sides of (59):

$$\begin{aligned} \nabla \times \nabla \times \left(\mathbf{E} - \frac{\mathbf{j}}{i\omega\epsilon_0}\right) &= k^2\mathbf{E} - i\omega\mu_0\mathbf{j} - \nabla \times \nabla \times \frac{\mathbf{j}}{i\omega\epsilon_0} \\ &= k^2\left(\mathbf{E} - \frac{\mathbf{j}}{i\omega\epsilon_0}\right) - \nabla \times \nabla \times \frac{\mathbf{j}}{i\omega\epsilon_0} \end{aligned} \tag{72}$$

Substitution of (71) into (72) yields the desired wave equation:

$$\nabla^2 \left(\mathbf{E} - \frac{\mathbf{j}}{i\omega\epsilon_0} \right) + k^2 \left(\mathbf{E} - \frac{\mathbf{j}}{i\omega\epsilon_0} \right) = \nabla \times \nabla \times \frac{\mathbf{j}}{i\omega\epsilon_0} \tag{73}$$

The same development can be made for $\mathbf{B}$ and the result would be:

$$\nabla^2 (\mathbf{B}) + k^2 (\mathbf{B}) = -\mu_0 \nabla \times \mathbf{j} \tag{74}$$

Equations (70), (73), (74) and $\nabla \cdot \mathbf{B} = 0$ together are proven to be equivalent to Maxwell's equations in free space (YAGHJIAN, 1980).

4.3.2 Solving the wave equation

Again we use the Green's function method for solving differential equation (73).

Using the Green's method for solving differential equations, we look for a function G such that:

$$\nabla^2 G + k^2 G = \delta \tag{75}$$

where δ is the Dirac's delta function. One may see that equation (75) was solved in section (4.1), so G is the same as found there.

We have then:

$$\left(\mathbf{E}(\mathbf{r}) - \mathbf{E}_{inc}(\mathbf{r}) - \frac{\mathbf{j}(\mathbf{r})}{i\omega\epsilon_0} \right) = \frac{1}{i\omega\epsilon_0} \int d^3 r' \left[\nabla \times \nabla \times \mathbf{j}(\mathbf{r}') \right] G(\mathbf{r}, \mathbf{r}') \tag{76}$$

4.3.3 Divide et impera

We use here the dielectric scatterer of volume V used in the beginning of the chapter. Hereafter, V will be used interchangeably to make reference to the scatterer itself or to the mathematical set if the points composing it.

We consider now another volume V_0 fully contained in V, so $V_0 \subset V$. This volume shall be always electrically small when compared to V.

Inside V_0 we choose an arbitrary point $\mathbf{r}_0$ as shown in Figure (2) and, fixing the shape of V_0 we can make it shrink around this point.

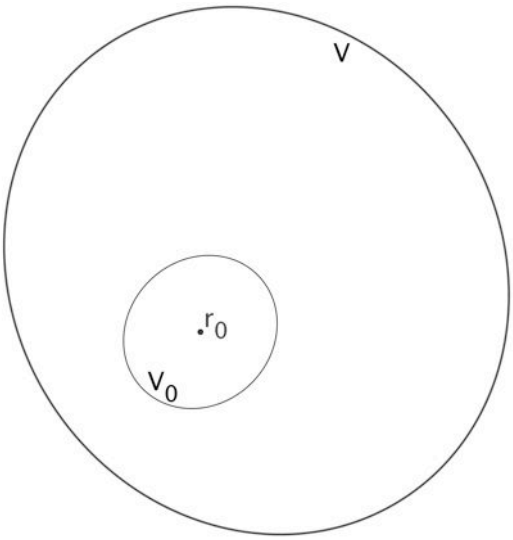

Figure 2: Decomposition of V in order to ease equation (50) calculation. Although here represented by ellipses, there are no constraints on the shapes of V and V_0.

We remove the singularity on (76) by simply taking out the volume V_0.

$$\left(\mathbf{E}(\mathbf{r}_0) - \mathbf{E}_{inc}(\mathbf{r}_0) - \frac{\mathbf{j}(\mathbf{r}_0)}{i\omega\epsilon_0}\right) = \frac{1}{i\omega\epsilon_0} \lim_{V_0 \to 0} \int_{V \setminus V_0} d^3r' \left[\nabla \times \nabla \times \mathbf{j}(\mathbf{r}')\right] G(\mathbf{r}_0, \mathbf{r}') \tag{77}$$

Now we recall the following vector identity, being ψ a scalar and $\mathbf{A}$ a vector:

$$\psi[\nabla \times \mathbf{A}] = \nabla \times (\psi\mathbf{A}) - \nabla\psi \times \mathbf{A} \tag{78}$$

We make $\psi = G$ and $\mathbf{A} = \nabla \times \mathbf{j}$:

$$G[\nabla \times \nabla \times \mathbf{j}] = \nabla \times (G\nabla \times \mathbf{j}) - \nabla G \times (\nabla \times \mathbf{j}) \tag{79}$$

We recall yet another vector identity and, being ∂V the boundary of a volume V and $\hat{\mathbf{n}}$ the outward normal to this volume:

$$\int_V (\nabla \times \mathbf{A}) dV = \int_{\partial V} (\hat{\mathbf{n}} \times \mathbf{A}) dS \tag{80}$$

Using (80) and (79) in (77):

$$\begin{aligned}
\left(\mathbf{E}-\mathbf{E}_{inc}-\frac{\mathbf{j}}{i\omega\epsilon_0}\right) &= \frac{1}{i\omega\epsilon_0}\lim_{V_0\to 0}\int_{V\setminus V_0} d^3r'\left[\nabla\times(G\nabla\times\mathbf{j})-\nabla G\times(\nabla\times\mathbf{j})\right] \\
&= \frac{1}{i\omega\epsilon_0}\left(\lim_{V_0\to 0}\int_{V\setminus V_0} d^3r'\left[\nabla\times(G\nabla\times\mathbf{j})\right]\right. \\
&\quad \left.-\lim_{V_0\to 0}\int_{V\setminus V_0} d^3r'\left[\nabla G\times(\nabla\times\mathbf{j})\right]\right) \\
&= \frac{1}{i\omega\epsilon_0}\left(\int_{\partial V} d^2r'\Big(\hat{\mathbf{n}}\times(G\nabla\times\mathbf{j})\Big)-\lim_{V_0\to 0}\int_{\partial V_0} d^2r'\Big(\hat{\mathbf{n}}\times(G\nabla\times\mathbf{j})\Big)\right. \\
&\quad \left.-\lim_{V_0\to 0}\int_{V\setminus V_0} d^3r'\left[\nabla G\times(\nabla\times\mathbf{j})\right]\right) \\
&= -\frac{1}{i\omega\epsilon_0}\lim_{V_0\to 0}\int_{V\setminus V_0} d^3r'\left[\nabla G\times(\nabla\times\mathbf{j})\right] \qquad (81)
\end{aligned}$$

Since V is chosen to lie outside the source region, the integral over this surface vanishes. The surface integral over ∂V_0 also vanishes because V_0 is shrinking and its surface varies as r^2 whereas the function being integrated, G, varies as $1/r$. As usual, $r=|r-r_0|$.

Now we use the fact that $\nabla\psi\times\mathbf{A}=(\nabla\times\psi\bar{\bar{\mathbf{I}}})\cdot\mathbf{A}$, where $\bar{\bar{\mathbf{I}}}$ is the unit dyadic:

$$\mathbf{E}-\mathbf{E}_{inc}=\frac{\mathbf{j}}{i\omega\epsilon_0}-\frac{1}{i\omega\epsilon_0}\lim_{V_0\to 0}\int_{V\setminus V_0} d^3r'\left[\left(\nabla\times G\bar{\bar{\mathbf{I}}}\right)\cdot\Big(\nabla\times\mathbf{j}\Big)\right] \qquad (82)$$

For convenience we will introduce $\bar{\bar{\mathbf{G}}}_m$ as $\bar{\bar{\mathbf{G}}}_m=(\nabla\times G\bar{\bar{\mathbf{I}}})$. It is easy to prove that $\bar{\bar{\mathbf{G}}}_m$ is the solution to the magnetic dyadic wave equation in free space. The development is analogous to the one done in section (4.2) and since we are interested in the electric field it will not be made here. Even if not proved, this fact justify the index m on $\bar{\bar{\mathbf{G}}}_m$, m standing for magnetic.

Proceeding with the development of equation (82):

$$\begin{aligned}
\mathbf{E}-\mathbf{E}_{inc}-\frac{\mathbf{j}}{i\omega\epsilon_0} &= -\frac{1}{i\omega\epsilon_0}\lim_{V_0\to 0}\int_{V\setminus V_0} d^3r'\bar{\bar{\mathbf{G}}}_m\cdot(\nabla\times\mathbf{j}) \\
&= \frac{1}{i\omega\epsilon_0}\lim_{V_0\to 0}\int_{V\setminus V_0} d^3r'(\nabla\cdot(\mathbf{j}\times\bar{\bar{\mathbf{G}}}_m)+\mathbf{j}\cdot\nabla\times\bar{\bar{\mathbf{G}}}_m) \\
&= \frac{1}{i\omega\epsilon_0}\lim_{V_0\to 0}\int_{V\setminus V_0} d^3r'(\mathbf{j}\cdot\nabla\times\bar{\bar{\mathbf{G}}}_m+\nabla\cdot(\mathbf{j}\times\bar{\bar{\mathbf{G}}}_m)) \\
&= \frac{1}{i\omega\epsilon_0}\left(\lim_{V_0\to 0}\int_{V\setminus V_0} d^3r'(\mathbf{j}\cdot\nabla\times\bar{\bar{\mathbf{G}}}_m)\right. \\
&\quad \left.+\lim_{V_0\to 0}\int_{\partial V_0} d^2r'((\bar{\bar{\mathbf{G}}}_m\times\hat{\mathbf{n}})\cdot\mathbf{j})\right) \qquad (83)
\end{aligned}$$

If we consider a constant current density within ∂V_0 the surface integral on (83) may be

simplified.

$$\begin{aligned}\int_{\partial V_0} d^2r'((\bar{\bar{\mathbf{G}}}_m \times \hat{\mathbf{n}}) \cdot \mathbf{j}) &= \int_{\partial V_0} d^2r'((\nabla \times \bar{\bar{\mathbf{I}}}) \times G\hat{\mathbf{n}}) \cdot \mathbf{j}) \\ &= -\mathbf{j} \cdot \int_{\partial V_0} d^2r'((\bar{\bar{\mathbf{I}}} \times \nabla G) \times \hat{\mathbf{n}})) \end{aligned} \tag{84}$$

Use has been made of dyadic identities found in appendix A.

If we calculate the gradient of the scalar Green's function G found in equation (58) we reach:

$$\nabla G = \left(ik - \frac{1'}{r}\right)\hat{\mathbf{r}}' \frac{\exp(ikr')}{4\pi r'} \tag{85}$$

where, as usual, r' is the distance between $\mathbf{r}$ and $\mathbf{r}'$ ($r' = |\mathbf{r} - \mathbf{r}'|$) and $\hat{r}'$ is the unitary vector pointing from $\mathbf{r}'$ to $\mathbf{r}$ ($\hat{\mathbf{r}}' = (\mathbf{r}' - \mathbf{r})/r'$).

Injecting (85) into (84):

$$\begin{aligned}\int_{\partial V_0} d^2r'((\bar{\bar{\mathbf{G}}}_m \times \hat{\mathbf{n}}) \cdot \mathbf{j}) &= -\mathbf{j} \cdot \int_{\partial V_0} d^2r' \left[\left(\bar{\bar{\mathbf{I}}} \times \left(ik - \frac{1'}{r}\right)\hat{\mathbf{r}}' \frac{\exp(ikr')}{4\pi r'}\right) \times \hat{\mathbf{n}}\right] \\ &= \mathbf{j} \cdot \frac{1}{4\pi} \int_{\partial V_0} d^2r' \left[\left(\bar{\bar{\mathbf{I}}} \times \frac{\hat{\mathbf{r}}'}{r'^2}\right) \times \hat{\mathbf{n}}\right] \\ &= \mathbf{j} \cdot \frac{1}{4\pi} \int_{\partial V_0} d^2r' \left(\frac{\hat{\mathbf{r}}'\hat{\mathbf{n}} - (\hat{\mathbf{r}}' \cdot \hat{\mathbf{n}})\bar{\mathbf{I}}}{r'^2}\right) \\ &= -\mathbf{j} \cdot \left[\bar{\bar{\mathbf{I}}} - \frac{1}{4\pi} \int_{\partial V_0} d^2r' \frac{\hat{\mathbf{r}}'\hat{\mathbf{n}}}{r'^2}\right] \end{aligned} \tag{86}$$

Some remarks must be made regarding the result obtained in (86). First, the limit $V_0 \to 0$ is implicit and that justifies why the term ik vanishes. Second,the integral of $\hat{\mathbf{r}}' \cdot \hat{\mathbf{n}}/(r'^2)$ over a surface is the definition of solid angle and the result of this integral is independent of the shape and size of V_0. Since we are integrating over the whole surface of V_0 the result is 4π.

To the remaining integral in (86) we give a special name: depolarization dyadic, noted $\bar{\bar{\mathbf{L}}}$. It is a simple exercise to prove that this dyadic is real, symmetric, that it has an unitary trace and also that its value is not dependent of the size of V_0, but only its shape. For a sphere this dyadic is diagonal with all elements equals to 1/3 - independently of the volume of the sphere.

In order to finish the analysis we combine equations (86), (84) and (83) reaching:

$$\mathbf{E} - \mathbf{E}_{inc} = \frac{1}{i\omega\epsilon_0}\left(\lim_{V_0 \to 0} \int_{V \setminus V_0} d^3r'(\mathbf{j} \cdot \nabla \times \bar{\bar{\mathbf{G}}}_m) + \bar{\bar{\mathbf{L}}} \cdot \mathbf{j}\right) \tag{87}$$

We introduce $\bar{\bar{\mathbf{G}}}_e = (-1/k^2)\nabla \times \bar{\bar{\mathbf{G}}}_m$. Similarly to $\bar{\bar{\mathbf{G}}}_m$, the e index is a reference to the electric field, meaning that $\bar{\bar{\mathbf{G}}}_e$ is the solution to the electric dyadic wave equation in free space. Since the dyadic wave equation in free space was solved in section (4.2) $\bar{\bar{\mathbf{G}}}_e$ must

be equal to $\bar{\bar{\mathbf{G}}}$. In fact,

$$\begin{aligned}
\bar{\bar{\mathbf{G}}}_e &= -\frac{1}{k^2}\nabla\times\bar{\bar{\mathbf{G}}}_m \\
&= --\frac{1}{k^2}\nabla\times\nabla\times G\bar{\bar{\mathbf{I}}} \\
&= -\frac{1}{k^2}\left[-\nabla^2(G\bar{\bar{\mathbf{I}}})+\nabla(\nabla\cdot G\bar{\bar{\mathbf{I}}})\right] \\
&= -\left(\bar{\bar{\mathbf{I}}}+\frac{1}{k^2}\nabla\nabla\right)G \\
&= \bar{\bar{\mathbf{G}}}
\end{aligned} \tag{88}$$

Using the fact that $\mathbf{j} = -i\omega\mathbf{P} = -i\omega\epsilon_0\chi\mathbf{E}$ and equation (88) in (87) we finally reach our desired equation.

$$\mathbf{E}(\mathbf{r}) = \mathbf{E}_{inc}(\mathbf{r}) + k^2\int_{V\setminus V_0}\bar{\bar{\mathbf{G}}}(\mathbf{r},\mathbf{r}')\chi(\mathbf{r}')\mathbf{E}(\mathbf{r}')d^3r' - \bar{\bar{\mathbf{L}}}(\partial V_0,\mathbf{r})\chi(\mathbf{r})\mathbf{E}(\mathbf{r}) \tag{89}$$

4.4 Remarks and conclusion

In this chapter important concepts were introduced, such as the Green's function and dyadic Green's function for free-space and the depolarization factor. The mathematical procedure for the singularity removal was made step by step so those concepts could appear naturally.

As well as understanding the mathematical development, it is essential to have a good understanding on how the singularity removal is done. The idea of using an *exclusion volume* where the sources are situated is the base for some homogenization techniques and will be the base for calculating the effective permittivity of a mixture here.

Equation (89) has a clear physical meaning - The electric field in a source region is the joint effect of the external field and one electric field that is dependent of the shape of the exclusion volume. The knowledge of free space dyadic Green's function alone is not sufficient for knowing the electric field at source regions.

The discretization of equation (89) will lead to the discrete dipole approximation formulation used in this dissertation. It is then the most relevant equation to yield the aimed result of calculating effective permittivity of mixtures using the DDA method.

Some useful properties of the depolarization factor, as well as values for several shapes are given in the Appendix B.

Chapter 5

The discrete dipole approximation

The discrete-dipole approximation (DDA) or coupled-dipole approximation is a computational method used mainly to compute scattering properties of arbitrarily-shaped bodies. It consists on the simple idea of dividing the scatterer in a finite number of dipoles. The dipoles interact with each other and with the illuminating electric field and, using the DDA method, the dipole moments of those dipoles may be calculated by solving a linear system (YURKIN; HOEKSTRA, 2007a).

This method was originally developed in the 70's by Purcell and Pennypacker(PURCELL; PENNYPACKER, 1973) to compute extinction cross-section and other scattering properties of interstellar dust. Composing dipoles in cubical cells and computing their interaction, they where able to find the dipole moments of those dipoles and then calculate the desired scattering properties. Even with the computational limitation, the results for spheres where close to that predicted theoretically by Mie theory. Besides its simple and highly intuitive formulation, the DDA approach became popular when scientists started sharing their software to the community. Draine and Flatau (DRAINE; FLATAU, 1994) were the first to make a free Fortran implementation of the DDA, named DDSCAT. Since then many other implementations such as ADDA (YURKIN; HOEKSTRA, 2011) by Yurkin, OpenDDA (DONALD; GOLDEN; JENNINGS, 2009) by Mc Donald and the MatLab Toolbox (LOKE; MENGÜÇ; NIEMINEN, 2011) by Loke were developed and great effort was done to improve the method accuracy (CHAUMET; RAHMANI, 2004), (CHAUMET; RAHMANI, 2009), (DRAINE; GOODMAN, 1993), (PILLER; MARTIN, 1998), (YURKIN; HOEKSTRA, 2007b), (YURKIN; MIN; HOEKSTRA, 2010).

In this chapter we are going to present the classical DDA formulation by discretizing equation (89). This formulation will be the basis for solving the mixture problem.

5.1 DDA formulation

We use the same conventions used in chapter (4).

Let V be a finite volume that contains all the problem's source points. The total electric field $\mathbf{E}$ inside one of those source points $V_0 \subset V$ is calculated by equation (89)(YURKIN; HOEKSTRA, 2007b).

$$\mathbf{E}(\mathbf{r}) = \mathbf{E}_{inc}(\mathbf{r}) + k^2 \int_{V \setminus V_0} \bar{\bar{\mathbf{G}}}(\mathbf{r}, \mathbf{r}')\chi(\mathbf{r}')\mathbf{E}(\mathbf{r}')d^3r' - \bar{\bar{\mathbf{L}}}(\partial V_0, \mathbf{r})\chi(\mathbf{r})\mathbf{E}(\mathbf{r}) \qquad \text{(89 revisited)}$$

The DDA formulation basis is the discretization of equation (89) making the right assumptions and considerations. Before starting the discretization we show the explicit expression for $k^2\bar{\bar{\mathbf{G}}}(\mathbf{r}, \mathbf{r}')$, that we will call hereafter $\bar{\bar{\mathbf{A}}}$ - the interaction matrix.

$$\bar{\bar{\mathbf{A}}}(\mathbf{r}, \mathbf{r}') = \frac{1}{4\pi} \cdot \frac{\exp(ikr')}{r'} \left[k^2(\hat{\mathbf{r}}'\hat{\mathbf{r}}' - \bar{\bar{\mathbf{I}}}) + \frac{ikr' - 1}{r'^2}(3\hat{\mathbf{r}}'\hat{\mathbf{r}}' - \bar{\bar{\mathbf{I}}}) \right] \tag{90}$$

where r' is the distance between $\mathbf{r}$ and $\mathbf{r}'$ and $\hat{\mathbf{r}}'$ is the unitary vector pointing from $\mathbf{r}'$ to $\mathbf{r}$.

5.1.1 Discretization

We divide the original volume in a finite number of smaller subsets that don't overlap. Those subsets will be called dipoles from now on.

$$\begin{aligned} V &= \cup V_i \\ V_i \cap V_j &= \emptyset, \qquad i \neq j \end{aligned} \tag{91}$$

The first step is to consider two different points $\mathbf{r}_j$ and $\mathbf{r}_k$ and write the Dyadic Green's function and depolarization factor expressions for those particular points:

$$\bar{\mathbf{L}}_j = \bar{\mathbf{L}}(\partial V_i, \mathbf{r}_j) = -\frac{1}{4\pi} \oint_{\partial V_0} \frac{\hat{\mathbf{n}}_k \cdot \hat{\mathbf{r}}_{jk}}{r_{jk}^3} d^2r_k, \qquad r_k \in V_0 \setminus \partial V_0 \tag{92}$$

$$\mathbf{A}_{\mathbf{jk_{j\neq k}}} = \frac{1}{4\pi} \cdot \frac{\exp(ikr_{jk})}{r_{jk}} \left[k^2(\hat{\mathbf{r}}_{jk}\hat{\mathbf{r}}_{jk} - \bar{\bar{\mathbf{I}}}) + \frac{ikr_{jk} - 1}{r_{jk}^2}(3\hat{\mathbf{r}}_{jk}\hat{\mathbf{r}}_{jk} - \bar{\bar{\mathbf{I}}}) \right] \tag{93}$$

Where $r_{jk} = |\mathbf{r}_j - \mathbf{r}_k|$, $\hat{r}_j k$ is the unitary vector pointing from $\mathbf{r}_j$ to $\mathbf{r}_k$ and $\hat{\mathbf{n}}_k$ is the outward normal unitary vector to the surface ∂V_0 at $\mathbf{r}_k$.

If we consider the one of the volumes V_i being electrically small, it is a fair assumption to consider $\mathbf{E}$ and χ constant inside this dipole. Hence:

$$\begin{aligned} \mathbf{E}(\mathbf{r}) &= \mathbf{E}_i, \ \forall r \in V_i \\ \chi(\mathbf{r}) &= \chi_i, \ \forall r \in V_i \end{aligned} \tag{94}$$

We make one dipole V_i as the exclusion V_0 used in chapter (4). Since V_i is small, two points $\mathbf{r}_{i_1}$ and $\mathbf{r}_{i_2}$ are close to each other and their distance to one point outside V_i.

If we have another yet small volume V_j this assumptions are also valid and we have:

$$|r_i - r'| \approx |r_i - r''| = \mathbf{r_{ij}},\ \forall r', r'' \in V_j \tag{95}$$

Hence:

$$\int_{V_j} d^3\mathbf{r}' \left[\bar{\bar{\mathbf{A}}}(\mathbf{r_i}, \mathbf{r}')\chi(\mathbf{r}')\mathbf{E}(\mathbf{r}')\right] \;=\; V_j \bar{\bar{\mathbf{A}}}_{ij}\chi(\mathbf{r_j})\mathbf{E}(\mathbf{r_j}) \tag{96}$$

Reinjecting equations (94) and (96) into (89):

$$\mathbf{E}_i = \mathbf{E}_{inc_i} + \sum_{j\neq i}\left[V_j \bar{\bar{\mathbf{A}}}_{ij}\chi_j\mathbf{E}_j\right] - \bar{\bar{\mathbf{L}}}_i\chi_i\mathbf{E}_i \tag{97}$$

Recalling the definition of the polarization density:

$$\mathbf{P}_i = \epsilon_0\chi_i\mathbf{E}_i \tag{98}$$

For one dipole, we can approximate its dipole moment by:

$$\mathbf{p}_i = V_i\epsilon_0\chi_i\mathbf{E}_i \tag{99}$$

Introducing the polarizability tensor defined by $\mathbf{p} = \alpha\mathbf{E}$ (SALSKI, 2012):

$$\bar{\bar{\alpha}}_i = V_i\chi_i[\bar{\bar{\mathbf{I}}} + \bar{\bar{\mathbf{L}}}_i\chi_i]^{-1} \tag{100}$$

we reach:

$$\mathbf{E}_{inc_i} = \frac{1}{\epsilon_0}\cdot\left((\bar{\alpha}_i)^{-1}\mathbf{p}_i + \sum_{j\neq i}\bar{\mathbf{A}}_{ij}\mathbf{p}_j\right) \tag{101}$$

Define:

$$\bar{\bar{\mathbf{A}}}' = \begin{cases} \bar{\bar{\alpha}}_i^{-1}, & i = j \\ \bar{\bar{\mathbf{A}}}_{ij}, & i \neq j \end{cases} \tag{102}$$

Hence we have the linear system

$$\mathbf{E}_{inc} = \frac{1}{\epsilon_0}\cdot\mathbf{A}'\mathbf{p} \tag{103}$$

with dipole moments as unknowns.

5.2 Remarks and conclusion

Solving the DDA problem means finding a set of vectors $\mathbf{p}$ such that (103) is verified. In order to make it possible the knowledge of three parameters are essential: the incident electric field, the geometrical position of the dipoles in the space and the polarizability of each dipole.

The linear system (103) is then a very practical and simple method for calculating the dipole moment of a set of interacting dipoles. The solution of this linear system is made usually through iterative methods such as the conjugate-gradient method or minimal residual method. Since $r_{ij} = r_{ji}$ the interaction matrix is symmetric and several optimization methods may be used (YURKIN; HOEKSTRA, 2007a), (GOODMAN et al., 1991). This method has been applied in a big range of problems from the Purcell and Pannypacker's work on interstellar dust scattering to the study of plasmon resonance (WAHBEH, 2011).

The next chapter will present the mixing problem and how to use the DDA to solve it.

Chapter 6

The mixing problem

Pure materials are difficult to find in nature. Usually they all contain a certain number of impurities that give a material particular characteristics. A good example is the snow: the snow is composed by, in a simple approximation, ice, air and water - it is a mixture of several materials in different volume fractions and all contribute differently to the macroscopic (or effective) properties of the snow such as color, permittivity, density and so on.

The mixing problem has as goal to calculate the effective permittivity of a mixture of several materials given the relative quantities of the components of this mixture. In our example of the snow - the mixing problem would be to calculate the permittivity of the snow knowing the dielectric properties of the water, ice and air present in the mixture as well as their volume fraction.

The idea of effective permittivity is based on the permittivity that is measured ignoring all the microscopic components of the mixture. It is the same permittivity 'sensed' by an incident wave impinging on a homogeneous body.

Knowing and describing with complete fidelity all the elements of a mixture is an extremely challenging, to not say impossible, task. Even if the description of all microscopic elements contributing to the macroscopic electric properties were known, the computation of all of those elements and their effect on the macroscopic properties of the mixture would be unfeasible. Simplified models are then made with appropriate considerations to attempt to solve this problem and to help to predict values we only know for sure when they are measured.

Those models are, of course, extremely dependent on the ratio of the typical size of the inclusions and the wavelength used since smaller the wavelength, more sensitive to small variations the measure will be. Therefore effective permittivity (or any other effective parameter) is meaningful in a long-wave limit. Most of the approximate formulas to solve the mixing problem, usually called mixing rules, are derived using quasi-static or static arguments (SIHVOLA, 1999).

A mixing rule usually has the goal to derive macroscopic properties of a mixture

knowing its microscopic composition and properties. Some important applications have, however, an inverse goal: knowing the macroscopic properties it seeks to know the microscopic composition. This is the case of the remote sensing problem and the very important material synthesis problem.

If, for example, one wants to produce a conductive ink with conventional dielectric ink and graphene, or if one wants to control the losses to an optical modulator introducing graphene impurities into the optical guide the mixing rule may be used to calculate beforehand what is the ideal composition to the desired result.

In this chapter we are going to present some basic definitions of problems dealing with mixture and the most used homogenization techniques and mixing rules.

We will also, as the target result of this dissertation, derive an expression using the DDA to calculate the effective permittivity of a mixture for an arbitrary number of phases and geometric distribution of the inclusions - what is not, in general, the case for usual mixing formulas.

6.1 Basic definitions

The introduction defined what we are going to understand as the effective permittivity of a mixture. It will be the permittivity of a homogeneous body somehow equivalent to the mixture.

In order to describe the mixture we need to know the dielectric properties of the bulk, or host material. For a given mixture, ϵ_h denote this quantity.

In the mixture we also have the inclusions, materials that are not host. If we have N kind of inclusions, ϵ_{inc_j} for $j \in 0, 1, ..., N$ denotes the permittivity of each inclusion.

The number of phases of a mixture is the number of different materials that can be find in that mixtures - counting bulk and inclusions. A biphasic mixture is then a mixture composed by one host and one type of inclusions, a three-phase mixture by one host and two types of inclusions and so on. A set of inclusions sharing the same electrical and geometrical properties are understood to be of the same type.

6.1.1 From vacuum to the host

The results that will be derived in this chapter have inclusions immersed in a host material that may or may not be the vacuum. All equations derived so far were, nevertheless, considering the free-space as host.

We will go around this problem by simply scaling all the physical quantities form the vacuum to the new host: $\epsilon_0 \to \epsilon_h$ and $\lambda_0 \to \lambda_0/\sqrt{\epsilon_h}$.

Care must be taken to convert properly relative permittivities such as ϵ_{inc}. The relative permittivity of the inclusions are relative to the vacuum and value such as the susceptibility must be calculated with the permittivity relative to the host. For the sake of clarity

we write the expression for the susceptibility of one inclusion and the Clausius-Mossotti equation (47) as examples.

$$\chi_i = \epsilon_i - 1 \rightarrow \chi_i = \frac{\epsilon_i - \epsilon_h}{\epsilon_h} \tag{104}$$

$$\frac{\epsilon - \epsilon_0}{\epsilon + 2\epsilon_0} = \frac{1}{3\epsilon_0}\sum_i N_i\alpha_i \rightarrow \frac{\epsilon - \epsilon_h}{\epsilon + 2\epsilon_h} = \frac{1}{3\epsilon_h}\sum_i N_i\alpha_i \tag{105}$$

6.2 Usual mixing formulas

Although study of electrostatic properties of materials date from ancient Greece, studies of dielectric properties of mixtures of several materials started to appear only in the nineteenth century with the already presented Clausius-Mossotti equation (SIHVOLA, 1999). This equation gives the effective permittivity in terms of the polarizability and the number of the molecules composing a dielectric body. Later, after the studies of the electromagnetic nature of light by Maxwell, Lorentz and Lorenz derived a similar equation showing that the refractive index is dependent of the volume of the test body.

Later, great scientists such as Rayleigh, Mie, Bruggeman and Maxwell Garnett had interest in solving similar problems.

This last name, James Clerk Maxwell Garnett, in his seminal paper (GARNETT, 1906), while studying the color of metallic films, derived a formula that is still widely used.

Maxwell Garnett's formula will be used in this dissertation as a gauge to the DDA method that will be deduced and for that reason it will be analyzed in more depth than any other mixing rule.

6.2.1 Maxwell Garnett mixing rule

Maxwell Garnett formula can be deduced without trouble considering spherical inclusions, using the Clausius-Mossotti formula and assuming that the mixture is diluted, i.e., that the volume fraction f of the inclusions is small implying N_i small.

A more generic derivation such as made by Salski (SALSKI, 2012) will be presented. The formula obtained will be valid for a diluted mixture ($f << 1$) where the inclusions are randomly distributed and there is no correlation between the inclusions positions inside the host, i.e., there is no preferred position for the inclusions. The inclusions must also be much smaller than the wavelength.

We first write the equation for the electric displacement vector. It defines the effective permittivity ϵ_{eff}. Here $\mathbf{E}$ is the macroscopic field, $\mathbf{E}_{loc}$ denotes the local field and $\mathbf{E}_{inc}$ the incident electric field.

$$\mathbf{D} = \epsilon_{eff}\mathbf{E} = \epsilon_h\mathbf{E} + \mathbf{P} \tag{106}$$

In a simplistic approximation we will consider that one inclusion is not affected by the scattered field by another one. In this case the local field is equal to the incident field.

$$\mathbf{E}_{loc} = \mathbf{E}_{inc} = \mathbf{E} + \frac{\bar{\bar{\mathbf{L}}}\mathbf{P}}{\epsilon_h} \tag{107}$$

Combining $\mathbf{p} = \bar{\bar{\alpha}}\mathbf{E}_{loc}$ and $\mathbf{P} = \sum_i N_i \mathbf{p}_i$ with equation (106):

$$\epsilon_{eff} = \epsilon_h \bar{\bar{\mathbf{I}}} + \sum_i N_i \bar{\bar{\alpha}}_i \left[\bar{\bar{\mathbf{I}}} - \frac{1}{\epsilon_h} \sum_i N_i \bar{\bar{\alpha}}_i \bar{\bar{\mathbf{L}}}_i \right]^{-1} \tag{108}$$

It is important to remark that ϵ_{eff} is a tensor as well as the polarizability and the depolarization tensor.

Equation (108) is Maxwell Garnett formula for a multiphase mixture.

Some modifications on Maxwell Garnett formula may be used to get around its validity hypothesis. One example is the formula derived by Salski (SALSKI, 2012) for a 2D inclusion's distribution.

6.3 Using DDA to solve the mixing problem

During the derivation of Maxwell Garnett formula we considered that there was no interaction between the inclusions.

Here we are going to approximate the inclusions as dipoles and we are going to use the DDA formulation to find the dipole moment of each one of those inclusions.

The assumptions are, for now, the same as in the section 5.1. The volume V is a statistically relevant sample of the mixture whose effective permittivity we want to calculate. This volume may be composed by one host and a finite number of inclusions. The inclusions may have different permittivities and geometries and they may be distributed arbitrarily inside V.

This is a fundamental difference between this method and Maxwell Garnett. While in Maxwell Garnett no preferred position for the inclusions is possible, here nothing is limiting the relative position of the inclusions, as exemplified in Figure 3. When using MG approximation we assume that the distribution of the inclusions within the volume V is random, uniform and non-correlated(MALLET; GUÉRIN; SENTENAC, 2005). If we restrict the inclusions distribution geometry, MG may be adapted for simpler cases(SALSKI, 2012), but it fails for a general case.

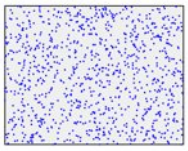

(a) Uniform and non-correlated

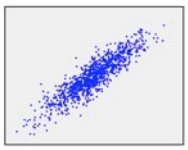

(b) Strongly correlated

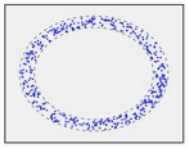

(c) Non-uniform probability distribution

Figure 3: Random distributions of inclusions within V. Maxwell-Garnett formula would be applicable only in (a) whereas the DDA approach can calculate the effective permittivity for any distribution of inclusions.

The volume V considered is finite and has a depolarization factor $\bar{\mathbf{L}}_h$. If we consider the volume a homogeneous body of permittivity ϵ_{eff}, the macroscopic field is calculated by:

$$\mathbf{E} = \mathbf{E}_{inc} - \frac{\bar{\bar{\mathbf{L}}}_h \cdot \mathbf{P}}{\epsilon_h} \tag{109}$$

We remember that the 'free-space' has now permittivity ϵ_h and that is why this value appears on equation (109).

We use now the definition of the effective permittivity given by equation (106). Solving it for ϵ_{eff} we obtain expresion (110).

$$\epsilon_{eff_j} = \epsilon_h + \frac{P_j}{E_{inc_j} - \frac{\left(\bar{\bar{\mathbf{L}}}_h \cdot \mathbf{P}\right)_j}{\epsilon_h}} \qquad j = x, y, z \tag{110}$$

The polarization $\mathbf{P}$ is linked to the dipole moments of the inclusions (JACKSON, 1999). Let n_i be the number of inclusions of type i, v_i its volume, $\langle p_i \rangle$ its average dipole moment and f_i its volume fraction. So:

$$\mathbf{P} = \frac{1}{V} \sum_i n_i \langle \mathbf{p}_i \rangle = \sum_i \frac{f_i}{v_i} \langle \mathbf{p}_i \rangle \tag{111}$$

Since DDA equation gives us the dipole moments of each inclusion, the right hand side of equation (110) is completely known and so is the effective permittivity.

6.3.1 Remarks

In the method presented above all inclusions are modeled as dipoles under multiple scattering of the incident electric field, i.e., all inclusions are not only excited by the external electric field, but also by the scattered field of the other dipoles. If the wavelength of the incident field is λ_0 in the air, inside V it is $\lambda_0 \backslash \sqrt{\epsilon_h}$ and this wavelength must be much greater then the inclusions characteristic size so that the dipolar approximation holds. Figure (4) exemplifies that a bad choice of wavelength may lead to unacceptable error.

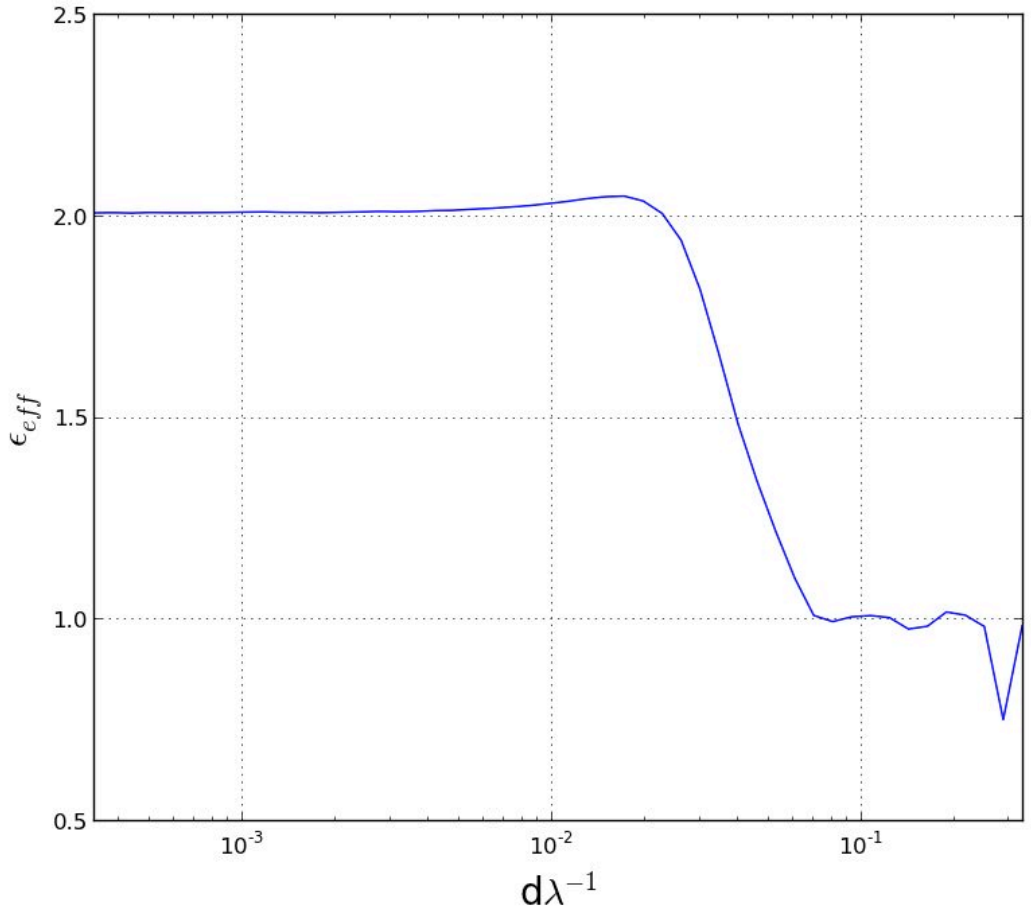

Figure 4: Effective permittivity calculated for a mixture of air (host) and spherical inclusions with $\epsilon_{inc} = 4$, diameter $d = 1mm$ and volume fraction $f = 50\%$. In the flat region of the curve, the quasi-static region, the inclusions can be approximated by dipoles and the method described here is applicable.

6.3.2 Equivalence with the Maxwell Garnett formula

If we consider that the mixture is very diluted the depolarization field of the host may be ignored and also that $\bar{\bar{\mathbf{A}}}_{ij} \approx 0$. Equation (110) becomes then:

$$\begin{aligned} \epsilon_{eff_j} &= \epsilon_h + \frac{P_j}{E_{inc_j}} \\ &= \epsilon_h + \frac{P_j}{E_{loc_j} - \frac{\left(\bar{\bar{\mathbf{L}}}_i \cdot \mathbf{P}\right)_j}{\epsilon_h}} \qquad j = x, y, z \end{aligned} \tag{112}$$

Equation (112) is the same as (108) and the results are consequently the same using both DDA or Maxwell Garnett mixing rule. We remark that in equation (112) E_{inc} refers to the incident electric field and that $\bar{\bar{\mathbf{L}}}_i$ refers to the inclusion depolarization dyadic.

Figure (5) shows that for small volume fractions ($f < 0.01$) there is a perfect agreement between the Maxwell Garnett and DDA results for spherical dielectric body with characteristics described in Table (1).

Frequency	1GHz
Wavelength	300mm
Number of points composing the sphere	3112
Geometry of the dipole	Spheres d=1mm
Lattice spacing	1mm
$\epsilon_h^{'}$	1
σ_h	0
σ_i	0
Polarizability	Simple
LS solving method	QMR (converged for all points)

Table 1: Parameters used to produce Figure 5

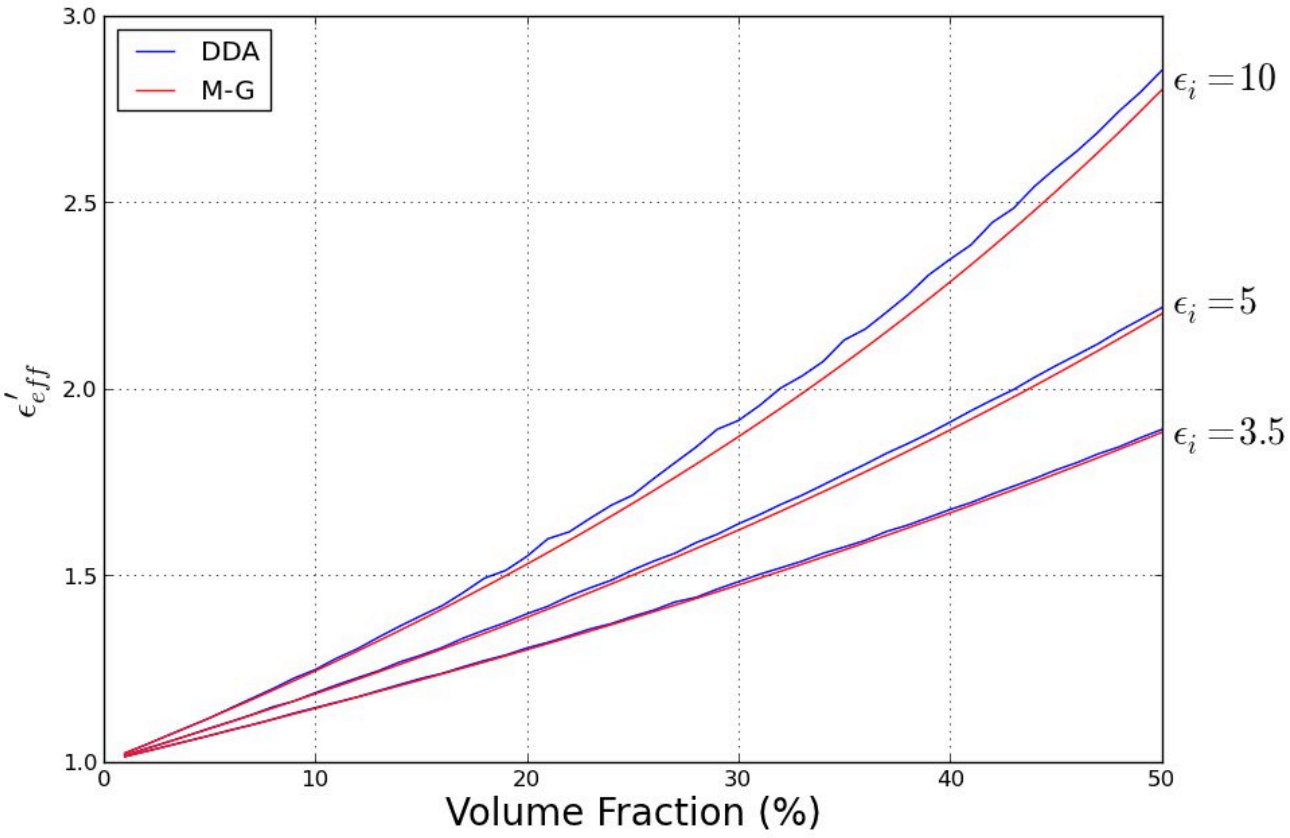

Figure 5: Comparison between MG and DDA results for a mixture described by Table 1. For low volume fractions the results given by both methods are rigorously the same.

6.3.3 Implementation

During the project two implementations of the DDA to calculate effective permitivitty were made. The first prototype was programmed based on Luke's MATLAB DDA implementation (LOKE; MENGÜÇ; NIEMINEN, 2011). As a final version a new implementation was made from scratch in C++ for faster calculations.

The inputs of the software are the necessary data to run the DDA: the geometrical characteristics of the inclusions as well of its positions inside the bulk, their permittivities and the permittivity of the host. Figure (6) shows how the calculation is performed.

If the input with inclusions positions is randomly generated a Monte-Carlo simulation should be performed. The final result is the average of each individual iteration result. As default, the code runs 500 iterations, but this value can be passed as an optional input.

It is important to note that all calculations are transparent to the final user, i.e., the user provide the inputs and get as result the effective permittivity. No intermediate step or extra calculation is needed.

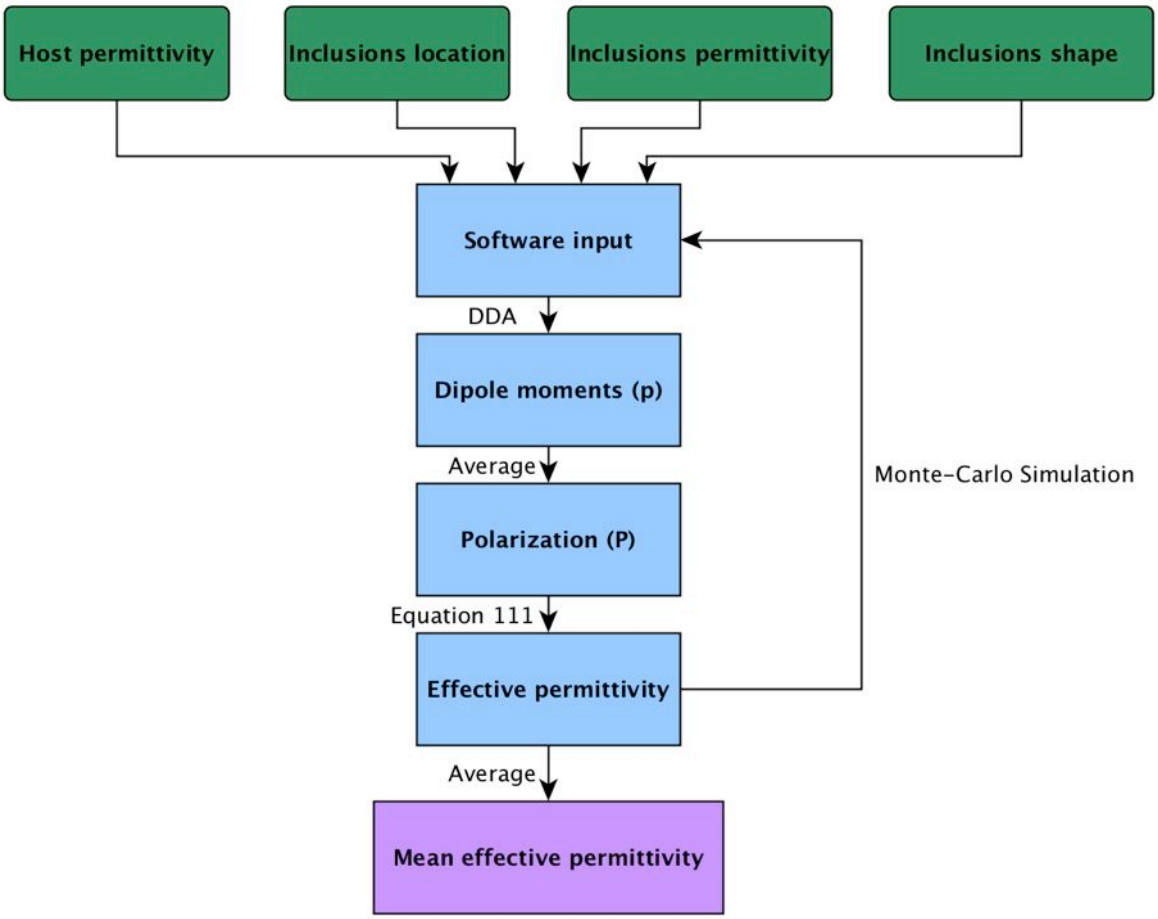

Figure 6: Simple diagram to exemplify how the implemented software works. The user give the inputs and the effective permittivity is returned.

6.3.4 Future improvements

Although coming from a very simple idea, the DDA method implementation can be improved to increase both accuracy and computational cost.

The list bellow is a compilation of ideas that were not yet tested but that should make the effective permittivity results closer to the expected.

- ❏ The inclusions are now treated each as a single dipole limiting the usage of the method in a quasi-static approximation. The inclusions may, however, be subdivided in spherical dipole clusters, what would be computationally costful yet more flexible.

- ❏ Now two inclusions never occupy the same space. This is not always true. Sometimes in a mixture two inclusions may be so close that they merge - it is the case for instance of a emulsion decanting or creaming. The implementation would be straightforward, if they share a point in space their depolarization factor is calculated for the merged structure and not for each individual inclusion.

- Using FFT to speed calculations as described by Purcell (GOODMAN; DRAINE; FLATAU, 1991).
- Use another Green's function such as the FCD (PILLER, 1999), (YURKIN; KANTER; HOEKSTRA, 2010)
- Add surface interaction to account for the reflected field on the interface of the test volume V

6.4 Conclusions

A method for calculating the effective permittivity has been derived from the DDA method. DDA is usually used for scattering studies and, to the best of the author knowledge, it has not been used for effective permittivity calculation so far although the derivation is simple and intuitive.

A brief proof of the equivalence of the Maxwell Garnett mixing formula and the DDA formulation when Maxwell Garnett validity hypothesis hold. A simple simulation showed that the results are almost the same in that case.

Since the implementation is still young, much has to be done to make it faster, more precise and more generic. The results so far are, nevertheless, promising as we shall see in the validation chapter.

Chapter 7

Validation of the proposed method

7.1 Comparison with the literature

Two papers were selected to put the proposed method into test. In the first presented, a mixture of epoxy and hollow glass microspheres, there are uncertainties on the permittivity of the epoxy resin used and also on the microspheres themselves. The results obtained were, however, closer to the experimental ones than the approximation given by the Maxwell-Garnett formula.

In the second selected case a much more complicated geometry and mixture is given. The inclusions are conductive and are not spheres, but fibers. In addition to that fact, the mixture is a thin epoxy film, which means that the fibers cannot rotate freely in all three dimensions, but only in two. Maxwell-Garnett in its original formulation cannot be used to solve this problem, but some modifications proposed by Salski (SALSKI, 2012) in Maxwell-Garnett's formula allow us to use it in this case. We will show that the proposed method, without any modification, had results almost as good as the modified Maxwell-Garnett and that making more appropriate approximations the results may be even better.

7.1.1 Hollow glass microspheres

Zhu et al. (ZHU et al., 2012) studied the dielectric properties of a mixture of hollow glass microspheres (HGM) immersed in an epoxy host. Those microspheres have a thin glass shell, their permittivity is estimated by a simple weighted mean, the properties of each sphere are shown in Table 2.

Type of HGM	Radius(μm)	ϵ_i	ϵ_h	$\sigma_h \left(\frac{S}{m}\right)$
K1	32.5	1.22	4.641	$1.28 \cdot 10^{-5}$
K20	32.5	1.36	4.641	$1.28 \cdot 10^{-5}$
S38HS	20	1.69	4.641	$1.28 \cdot 10^{-5}$
S60HS	15	2.10	4.641	$1.28 \cdot 10^{-5}$

Table 2: HGMs properties

In the original paper, the measures were compared to Maxwell-Garnett results. Here we compare the measurements with Maxwell-Garnett and DDA results and, as one may see in the figures bellow, for all HGMs, DDA results were, in general, closer to the experimental ones than MG.

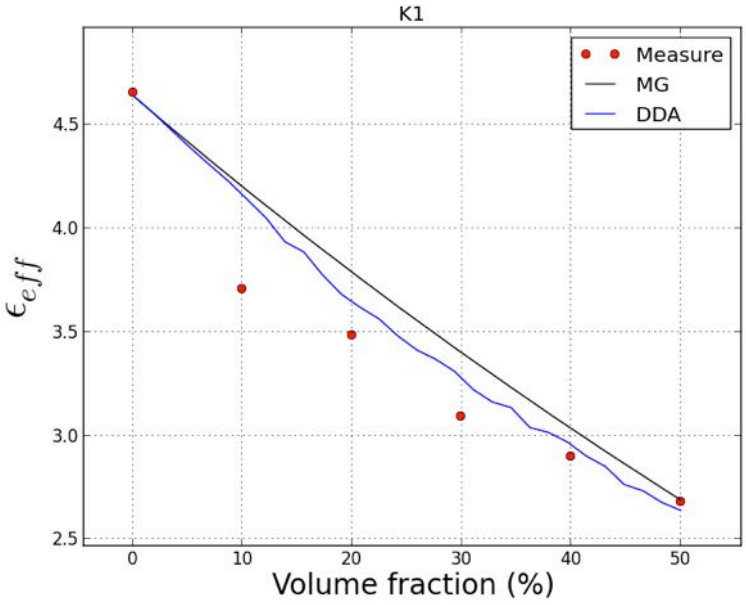

Figure 7: Hollow glass microspheres K1 inside an epoxy matrix. Comparison between Maxwell Garnett, DDA and measurements

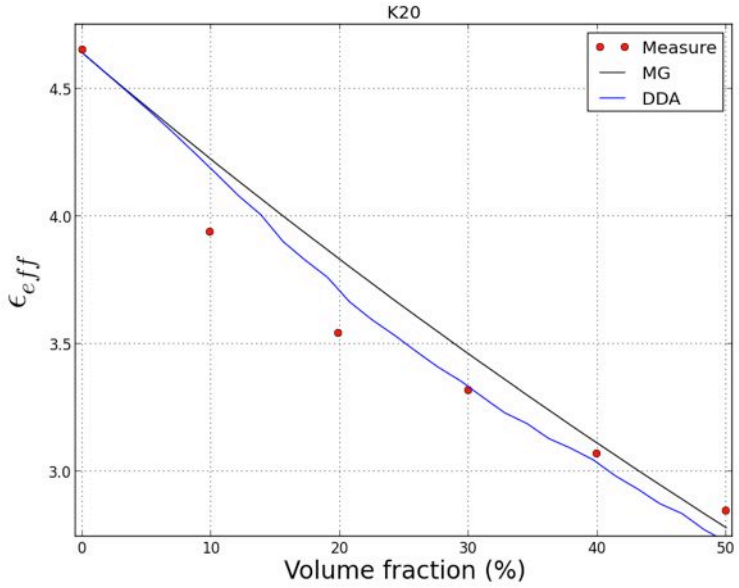

Figure 8: Hollow glass microspheres K20 inside an epoxy matrix. Comparison between Maxwell Garnett, DDA and measurements

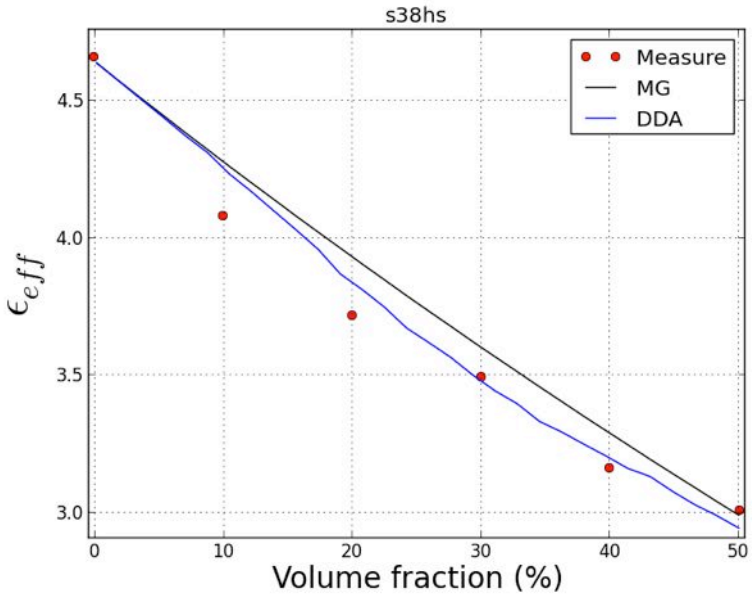

Figure 9: Hollow glass microspheres S38HS inside an epoxy matrix. Comparison between Maxwell Garnett, DDA and measurements

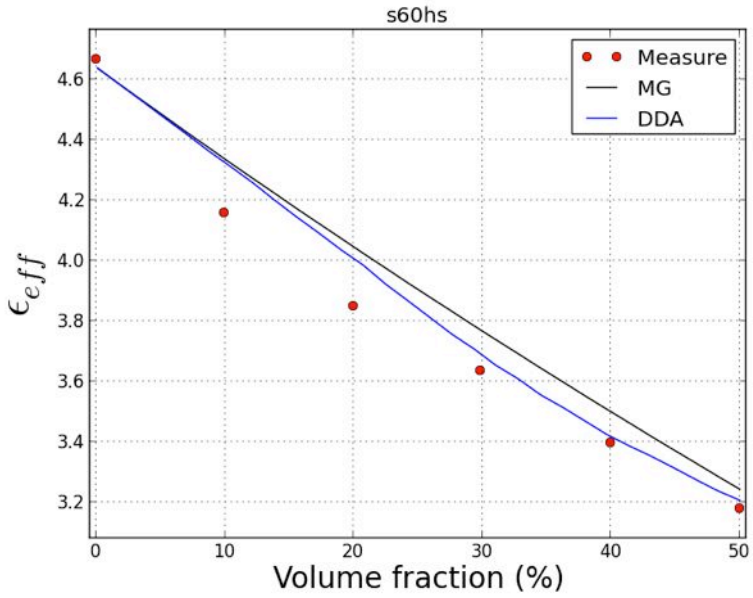

Figure 10: Hollow glass microspheres S60HS inside an epoxy matrix. Comparison between Maxwell Garnett, DDA and measurements

7.1.2 Carbon fibers

In (ROSA; MANCINELLI; SARASINI, 2009) studies were made in a epoxy film filled with carbon fibers. The complex effective permittivity was measured and the result compared to Maxwell-Garnett's predictions with a suitable correction for the geometrical restriction The characteristics of the film and the inclusions are presented in Table 3.

Epoxy permittivity	3
Film thickness	$550\mu m$
Fiber length	l=4mm
Fiber diameter	d=$7\mu m$
Fiber permittivity	2
Fiber conductivity	$\sigma_f = 40kS/m$
Fiber volume fraction	$f_i = 2.8 \cdot 10^{-4}$

Table 3: Characteristics of the films studied in (ROSA; MANCINELLI; SARASINI, 2009)

For convenience and ease of calculation of the depolarization dyadic, the shape of the fibers was approximated by ellipsoids with same aspect ratio and same electrical properties. The position of each inclusion was randomly selected as well as its orientation on the xy plane since the film is thinner than the length of the fibers, allowing rotations only in one direction.

Figure 11 shows the comparison between the results obtained with DDA, Maxwell-Garnett and the measurements.

As expected, in the y direction the permittivity was almost equal to that obtained for the x direction and in the z direction the permittivity was close to that of the host material.

The DDA method had fairly accurate results without any modification, as needed for the MG formula to work in this case. The accuracy of the DDA may increase if the fibers are considered as thin cylinders instead of ellipsoids and if small random elevation angles are allowed.

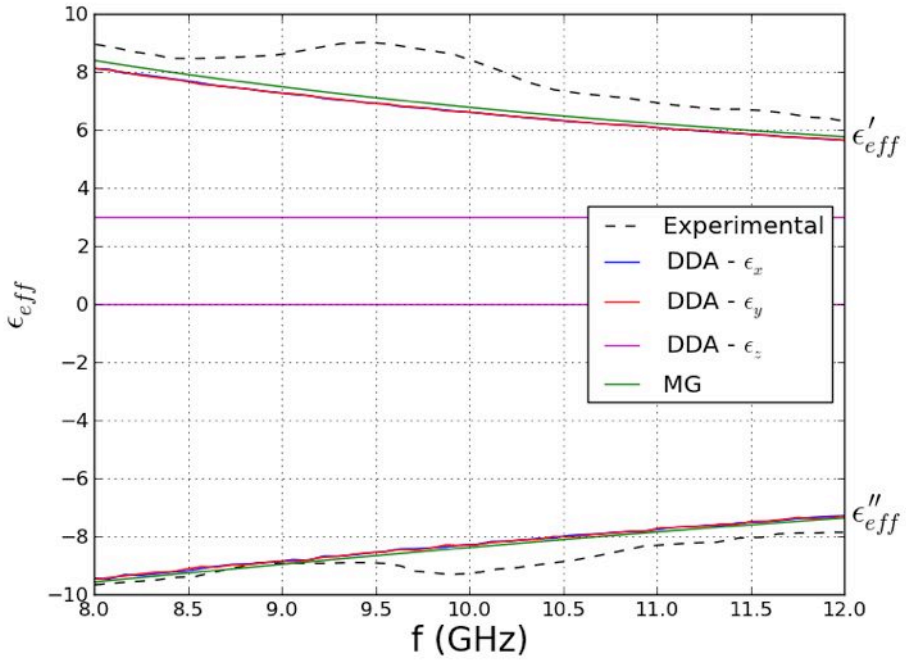

Figure 11: Experimental data, DDA and Maxwell Garnett results for an epoxy film with carbon fibers following the specifications in Table 3

7.2 Comparison with experiments

In order to validate the proposed method several samples of mixtures of a resin and other known materials were made. The experimental setup consisted essentially of a rectangular waveguide with cutting frequency of 6.4GHz, sample holders that would be attached to the waveguide setup, the samples and one Rohde&Schwarz ZVA 40 vector network analyzer(VNA). More details on the setup may be found on Appendix D.

All samples were tested in X-band frequencies - between 8Ghz and 12GHz and the S-parameters measured by VNA were used for the effective permittivity using the method described on Appendix C.

7.2.1 The host material

A vegetable oil-based polyurethane (PU) derived from castor oil plants was used as host material. In order to produce the resin two components must be added, one yellow (component A, figure (12)) and one brown (component B, figure(13)) - no details on the composition of those two parts were given by the vendor. Mixing the two parts in a proportion of 2xA parts for each component B part gives origin to a firm yellow resin (Figure 14), with an approximate density of $1.05 g/cm^3$.

Figure 12: Component A used to make the vegetable oil-base PU resin used as host material for the studied mixtures.

Figure 13: Component B used to make the vegetable oil-base PU resin used as host material for the studied mixtures.

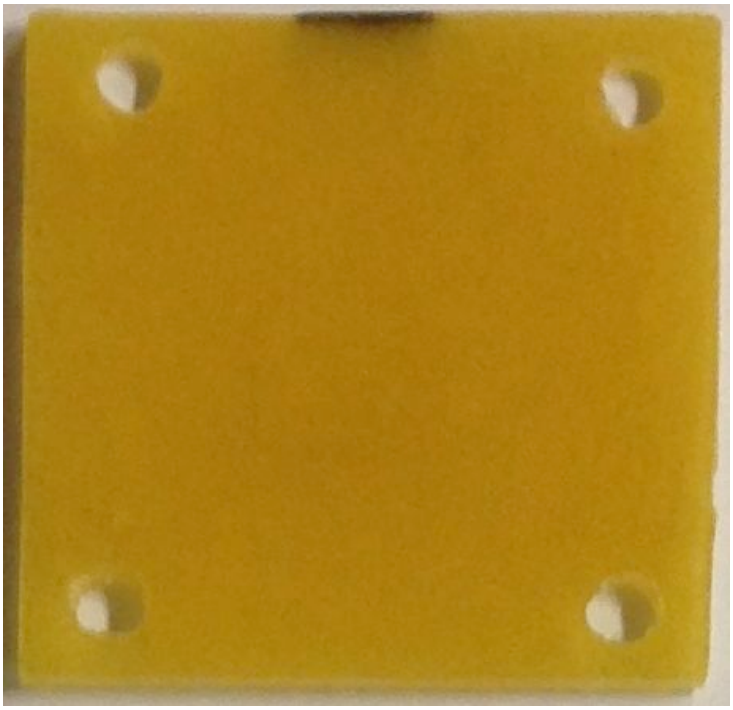

Figure 14: PU resin after 24 hours curing.

7.2.1.1 Making the resin

The mixture of components A and B is exothermic and become sticky after approximately 2 minutes. Care must be taken so the mixture do not become bubbly - mixing with a stick after the first minute increased enormously the number of bubbles in the final resin. The best approach found was to mix the components with a stick and depose it in a transparency sheet in a flat surface or inside the holder and cover it with a polyethylene (trash) bag. Although the first one generated a block of resin with thickness variations on the borders that method was preferred since the bubbles generated could go out of the resin during the curing process. Since in the second method the mixture is confined during the curing process, the bubbles do not have where to go out and stay in the mixture. As we will see later, bubbles are sometimes desired and this method is then also useful. The total curing process time took about one day for each batch of samples that was made.

7.2.2 Mixtures

Several mixtures were made adding new components to the resin before the curing process or inducing bubbles. The dimensions of the samples were cut to fit the sample holder and the unavoidable air gaps were compensated by an algorithm described on Appendix C. Several holders were used in order to have a good match between the thickness of the sample and the thickness of the sample holder - all the holders are listed on Appendix D.

Table 4 is a synthesis of the samples that were made and the characteristics of the inclusions.

Samples mixing ferrite powder and the base resin and also graphite powder and the base resin were produced but will not be presented here in the first version of this document due to time constraints. We are going then to focus on the sample with air inclusions.

Table 4: List of all the samples analyzed with the inclusions characteristics

Sample	Inclusion	Volume Fraction (%)	ϵ_r@10GHz	Shape	Comments
PU1	none	-	-	-	$\epsilon_h = 2.31$@10GHz
PU2	none	-	-	-	$\epsilon_h = 2.46$@10GHz
PU3	none	-	-	-	$\epsilon_h = 2.39$@10GHz
PU4	none	-	-	-	$\epsilon_h = 2.37$@10GHz
Air1	Air	3.9	1	spheres	non-uniform distribution

7.2.3 Dielectric properties of the resin

Based on measures done for the samples PUx,$x \in 1...4$, the average permittivity of the PU resin used is given by Figure (15).

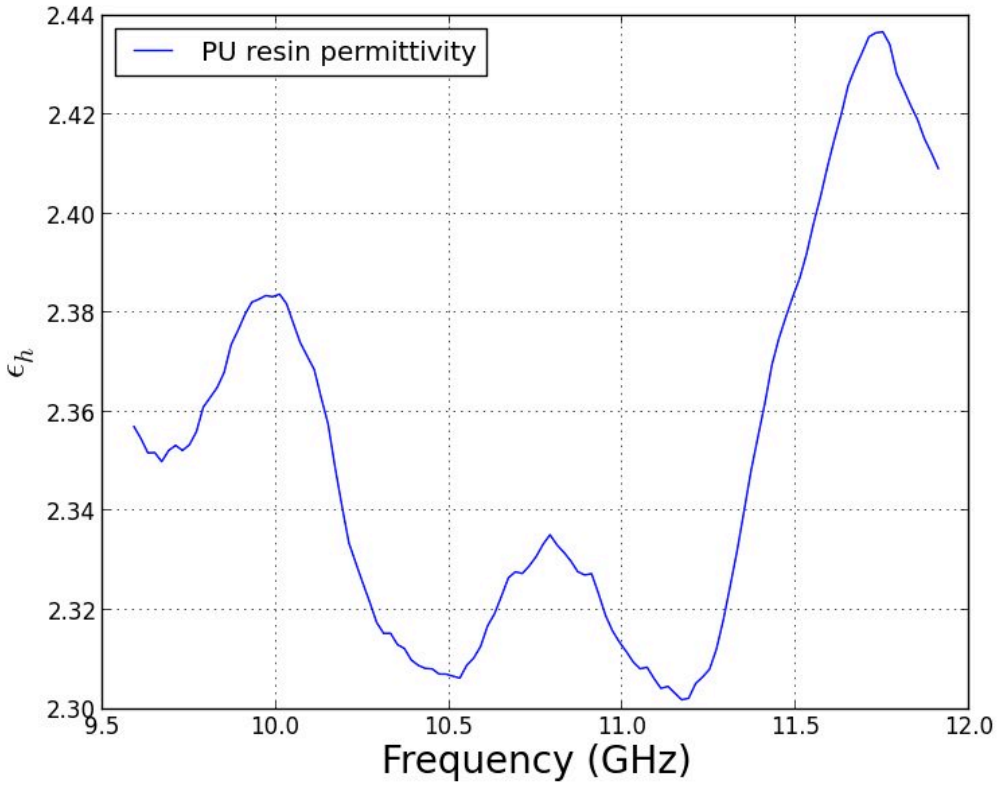

Figure 15: Effective permittivity of the PU resin used as host. Average over 4 samples.

7.2.4 Air1 sample

The first mixture to be studied is a mixture of PU and air bubbles. The air bubbles are not evenly distributed in the sample, they are concentrated in a area in its middle that is approximately circular (Figure (16)).

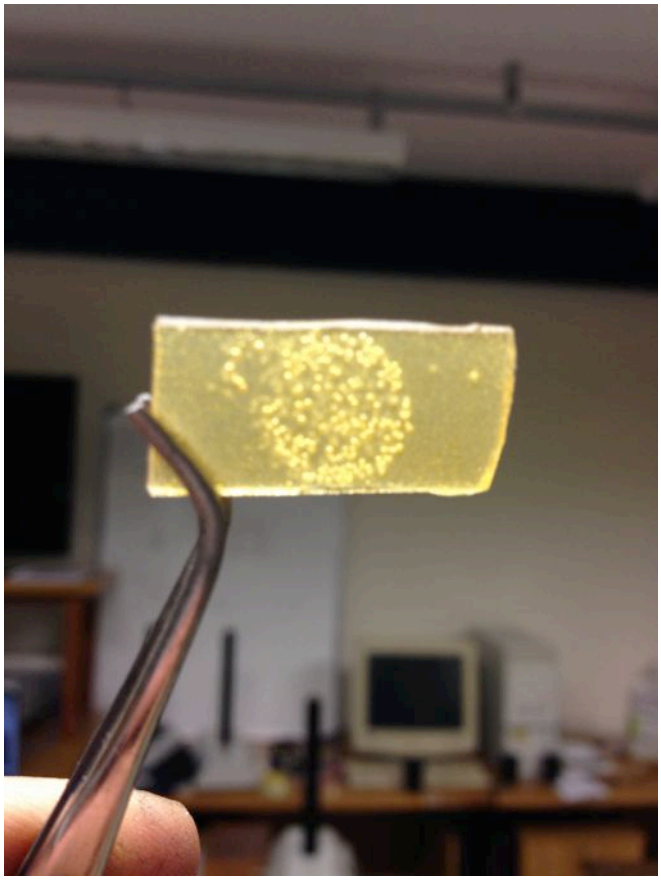

Figure 16: Sample Air1. The air bubbles are not distributed within all volume of the sample. They are approximately distributed in a circle in the middle of the sample.

Since the creation of the bubbles is not a controlled process, its volume fraction f must be indirectly measured after the resin is cured.

The density of the mixture is given by:

$$\begin{aligned} \rho_{mix} &= \frac{m_{air} + m_{PU}}{V_{air} + V_{PU}} \\ &= \frac{\rho_{PU} + \rho_{air} f}{1 + f} \end{aligned} \tag{113}$$

Hence:

$$f = \frac{\rho_{PU} - \rho_{mix}}{\rho_{mix} - \rho_{air}} \tag{114}$$

Since all those quantities are known, f can be calculated. In this case $\rho_{PU} = 1.05 g/cm^3$, $\rho_{mix} = 1.01 g/cm^3$ and $\rho_{air} = 0.001225 g/cm^3$ and then $f = 3.9\%$. Using a computer

vision algorithm we can process an image of the sample and extract the typical size of the bubbles.

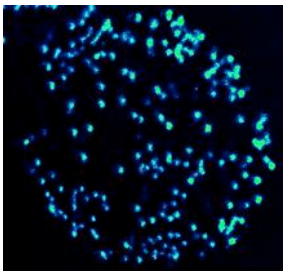

Figure 17: Colorized and zoomed air bubbles in sample Air1. Using a computer vision algorithm it is possible to extract the typical size of a bubble. In this case the typical diameter of the spheres is 0.559mm.

We compare the measure of the effective permittivity with the calculations made by using the DDA method and Maxwell Garnett mixing formula. Instead of a Monte Carlo simulation as done in the case of the carbon fibers, here only one solution was taken. The solution for a low volume fraction takes no more then a few seconds when solved in any modern computer.

We may note that, in general, the DDA results and Maxwell Garnett have a similar behavior. The DDA method is, however, more precise around 10GHz and 11.7Ghz (Figure 18). Even for a single calculation, and not an average, the results are close to what is expected.

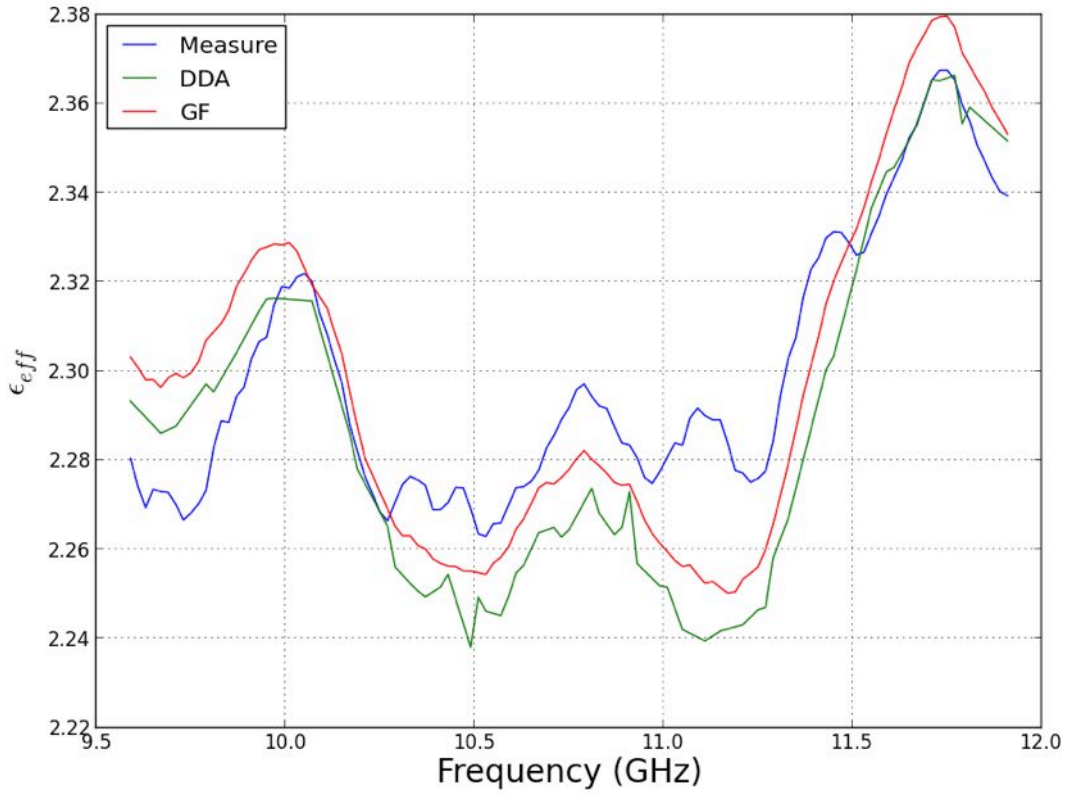

Figure 18: Comparison between DDA, MG and measured results for a mixture composed by PU and air with 3.9% volume fraction.

Conclusion

Although the calculation of the permittivity of mixtures and homogenization problems have been explored for more than one century, they are still a rich research domain. Classical approximate formulas have been modified to fit to specific problems and numerical methods have been used when a more general approach is needed. The proposed method is a mix between an analytical and computational method and it aims to be general and computationally efficient by making the appropriated assumptions and approximations. Before presenting the main result and its validation, a synthesis is made on Maxwell's equations in a material media and on Green's functions to solve the wave equation in free space. This second problem was explored in depth and one expression was derived by removing the singularity of the dyadic Green's function in a source region, this equation is then used to reach the final expression used in the usual discrete dipole approximation. A simple formula and intuitive formula was then derived and experimental data was gathered and compared to the results given by the proposed method.

The studies made here show the path to explore the mixing problem using the classical tools and also gives new paths to may lead to very promising results. Even if many improvements must be done to increase the accuracy of DDA for effective permittivity calculation and to theoretically set bounds for where the method is valid, the comparison between experimental and theoretical data shows clearly that for rough approximations the method is valid and, due to its high simplicity, easy to understand and use.

Bibliography

BLADEL, J. G. V. **Electromagnetic fields**. [S.l.]: John Wiley & Sons, 2007.

CHAUMET, P. C.; RAHMANI, A. Coupled dipole method for scatterers with large permittivity. **Physical Review E**, 2004. v. 70, n. 3, p. 036606, set. 2004.

_____. Coupled-dipole method for magnetic and negative-refraction materials. **Journal of Quantitative Spectroscopy & Radiative Transfer**, 2009. v. 110, n. 1-2, p. 22–29, jan. 2009.

DONALD, J. M.; GOLDEN, A.; JENNINGS, S. G. Opendda: a Novel High-Performance Computational Framework for the Discrete Dipole Approximation. **arXiv.org**, 2009. ago. 2009.

DRAINE, B. T.; FLATAU, P. J. Discrete-dipole approximation for scattering calculations. **Journal of the Optical Society of America A: Optic s and Image Science (ISSN 0740-3232)**, 1994. v. 11, p. 1491–1499, abr. 1994.

DRAINE, B. T.; GOODMAN, J. Beyond Clausius-Mossotti - Wave propagation on a polarizable point lattice and the discrete dipole approximation. **Astrophysical Journal**, 1993. v. 405, p. 685–697, mar. 1993.

GARNETT, J. M. Colours in metal glasses, in metallic films, and in metallic solutions. ii. **Philosophical Transactions of the Royal Society of London. Series A, Containing Papers of a Mathematical or Physical Character**, 1906. JSTOR, p. 237–288, 1906.

GOODMAN, J. et al. Application of fast-fourier-transform techniques to the discrete-dipole approximation. **Opt. Lett**, 1991. v. 16, n. 15, p. 1198–1200, 1991.

GOODMAN, J. J.; DRAINE, B. T.; FLATAU, P. J. Application of fast-Fourier-transform techniques to the discrete-dipole approximation. **Optics Letters**, 1991. v. 16, n. 1, p. 1198–1200, ago. 1991.

GUIO, P. Levi-civita symbol and cross product vector/tensor. 2011. 2011. Disponível em: <http://www.ucl.ac.uk/˜ucappgu/seminars/levi-civita.pdf>.

JACKSON, J. D. **Classical electrodynamics**. 3rd ed.. ed. New York, NY: Wiley, 1999. ISBN 9780471309321. Disponível em: <http://cdsweb.cern.ch/record/490457>.

KUEK, C. Measurement of dielectric material properties. **Rohde & Schwarz Application Note, RAC0607-0019**, 2006. 2006.

LAKHTAKIA, A. Strong and weak forms of the method of moments and the coupled dipole method for scattering of time-harmonic electromagnetic fields. **International Journal of Modern Physics C**, 1992. World Scientific, v. 3, n. 03, p. 583–603, 1992.

LOKE, V. L. Y.; MENGÜÇ, M. P.; NIEMINEN, T. A. Discrete-dipole approximation with surface interaction: Computational toolbox for MATLAB. **Journal of Quantitative Spectroscopy & Radiative Transfer**, 2011. v. 112, p. 1711–1725, jul. 2011.

MALLET, P.; GUÉRIN, C.-A.; SENTENAC, A. Maxwell-garnett mixing rule in the presence of multiple scattering: Derivation and accuracy. **Physical Review B**, 2005. APS, v. 72, n. 1, p. 014205, 2005.

MARQUIER, F. **Electromagnetisme**. Palaiseau, France: Institut d'Optique Graduate School, 2012.

NICOLSON, A.; ROSS, G. Measurement of the intrinsic properties of materials by time-domain techniques. **Instrumentation and Measurement, IEEE Transactions on**, 1970. IEEE, v. 19, n. 4, p. 377–382, 1970.

NITSCH, F. G. J.; WOLLENBERG, G. **Radiating Nonuniform Transmissionline Systems and the Partial Element Equivalent Circuit Method**. [S.l.]: John Wiley & Sons, 2009. ISBN 9780470845363.

NOTE, A. Agilent basics of measuring the dielectric properties of materials. **Agilent Literature Number**, 2006. 2006.

PAULA, A. L. de; BARROSO, J.; REZENDE, M. Modified nicolson-ross-weir (nrw) method to retrieve the constitutive parameters of low-loss materials. In: IEEE. **Microwave & Optoelectronics Conference (IMOC), 2011 SBMO/IEEE MTT-S International**. [S.l.], 2011. p. 488–492.

PILLER, N. B. Coupled-dipole approximation for high permittivity materials. **Optics Communications**, 1999. v. 160, p. 10–14, fev. 1999.

PILLER, N. B.; MARTIN, O. J. F. Increasing the performance of the coupled-dipole approximation: a spectral approach. **IEEE Transactions on Antennas and Propagation**, 1998. v. 46, n. 8, p. 1126–1137, 1998.

PURCELL, E. M.; PENNYPACKER, C. R. Scattering and Absorption of Light by Nonspherical Dielectric Grains. **Astrophysical Journal**, 1973. v. 186, p. 705–714, dez. 1973.

ROSA, I. M. D.; MANCINELLI, R.; SARASINI, F. Electromagnetic Design and Realization of Innovative Fiber-Reinforced Broad-Band Absorbing Screens. **IEEE Transactions on Electromagnetic Compatibility**, 2009. v. 51, ago. 2009.

SALSKI, B. The Extension of the Maxwell Garnett Mixing Rule for Dielectric Composites with Nonuniform Orientation of Ellipsoidal Inclusions. **Progress In Electromagnetics Research Letters**, 2012. v. 30, p. 173–184, 2012.

SCHEY, H. **Div, Grad, Curl, and all that: an informal text on vector calculus**. [S.l.]: W.W. Norton & Company, 1973.

SIHVOLA, A. H. **Electromagnetic mixing formulas and applications**. [S.l.]: Iet, 1999.

TSYMBAL, E. Y. **Dielectric properties of insulators**. 2013. Disponível em: <http://unlcms.unl.edu/cas/physics/tsymbal/teaching/SSP-927-/Section%2014_Dielectric_Properties_of_Insulators.pdf>.

WAHBEH, M. **Discrete-Dipole-Approximation (DDA) study of the plasmon resonance in single and coupled spherical silver nanoparticles in various configurations**. Tese (Doutorado) — Concordia University, 2011.

YAGHJIAN, A. D. Electric dyadic green's functions in the source region. **Proceedings of the IEEE**, 1980. IEEE, v. 68, n. 2, p. 248–263, 1980.

YORK, R. A. **Vector and Dyadic Analysis**. 2012. Disponível em: <http://my.ece-.ucsb.edu/York/Bobsclass/201B/W01/vectors.pdf>.

YURKIN, M. A.; HOEKSTRA, A. G. The discrete dipole approximation: an overview and recent developments. **Journal of Quantitative Spectroscopy and Radiative Transfer**, 2007. Elsevier, v. 106, n. 1, p. 558–589, 2007.

_____. The discrete dipole approximation: an overview and recent developments. **arXiv.org**, 2007. n. 1, p. 558–589, mar. 2007.

_____. The discrete-dipole-approximation code adda: capabilities and known limitations. **Journal of Quantitative Spectroscopy and Radiative Transfer**, 2011. Elsevier, v. 112, n. 13, p. 2234–2247, 2011.

YURKIN, M. A.; KANTER, D. D.; HOEKSTRA, A. G. Accuracy of the discrete dipole approximation for simulation of optical properties of gold nanoparticles. **Journal of Nanophotonics**, 2010. International Society for Optics and Photonics, v. 4, n. 1, p. 041585–041585, 2010.

YURKIN, M. A.; MIN, M.; HOEKSTRA, A. G. Application of the discrete dipole approximation to very large refractive indices: Filtered coupled dipoles revived. **Physical Review E**, 2010. v. 82, n. 3, p. 36703, set. 2010.

ZHU, B. et al. Thermal, dielectric and compressive properties of hollow glass microsphere filled epoxy-matrix composites. **Journal of Reinforced Plastics and Composites**, 2012. v. 31, n. 19, p. 1311–1326, out. 2012.

Appendix

APPENDIX **A**

Vector and tensor identities

This appendix aims to be a summary of the useful identities used throughout the text and to clarify the vector and dyadic/tensorial notation used. The Einstein notation and the Levi-Civita symbol are introduced and used to prove some of the identities. A more exhaustive list of identities may be found in (NITSCH; WOLLENBERG, 2009), (SCHEY, 1973), (GUIO, 2011), (YORK, 2012).

A.1 Notation

In this appendix and through the text the following notation is used:

- ψ - Scalar functions are represented by non-bold and non-italic characters
- $\mathbf{A}, \mathbf{a}$ - Vectors are represented by bold characters
- $\bar{\bar{\mathbf{D}}}$ - Dyadic tensors are represented by bold capital letters with a double bar
- $\hat{\mathbf{n}}$ - Unitary vectors are represented in small letters with a hat
- $\hat{\mathbf{e}}_i$ - A basis vector is represented be the letter e

A.2 The Levi-Civita symbol

The Levi-Civita symbol is a tensor of order 3 that is defined by:

$$\varepsilon_{ijk} = \begin{cases} 0, & \text{if } i = j \text{ or } i = k \text{ or } j = k \\ 1, & \text{if } ijk \text{ is a cyclic permutation of 1, 2, 3} \\ -1, & \text{if } ijk \text{ is a anti-cyclic permutation of 1, 2, 3} \end{cases} \tag{115}$$

Example:

$$\begin{aligned} \varepsilon_{iik} &= 0 \\ \varepsilon_{ijk} = \varepsilon kij &= 1 \\ \varepsilon_{kji} &= -1 \end{aligned}$$

A.2.1 Properties

The Kronecker delta is defined by:

$$\delta_{ij} = \begin{cases} 0, & \text{if } i \neq j \\ 1, & \text{if } i = j \end{cases} \tag{116}$$

The Levi-Civita tensor can be written in terms of the Kronecker delta.

$$\varepsilon_{ijk}\varepsilon_{imn} = \delta_{jm}\delta_{kn} - \delta_{jn}\delta_{km} \tag{117}$$

A.3 Einstein notation

The standard vector notation is:

$$\mathbf{A} = \sum_i a_i \hat{e}_i$$

In Einstein notation the summation symbol is implicit so:

$$\mathbf{A} = a_i \hat{e}_i$$

Dyadic tensors are the made by two juxtaposing vectors.

$$\bar{\bar{\mathbf{D}}} = D_{ij}\hat{\mathbf{e}}_i\hat{\mathbf{e}}_j = a_i b_j \hat{\mathbf{e}}_i\hat{\mathbf{e}}_j$$

The transpose of a dyadic tensor is

$$\bar{\bar{\mathbf{D}}}^T = D_{ji}\hat{\mathbf{e}}_j\hat{\mathbf{e}}_i = a_j b_i \hat{\mathbf{e}}_j\hat{\mathbf{e}}_i$$

And its trace:

$$Tr\left[\bar{\bar{\mathbf{D}}}\right] = \sum_{i=j} a_i b_j \hat{\mathbf{e}}_i\hat{\mathbf{e}}_j = \mathbf{A}\cdot\mathbf{B} \tag{118}$$

Where $\mathbf{A}$ and $\mathbf{B}$ are the vectors composing the dyadic.

A.3.1 Differential operators and usual operations using the Einstein notation

$$\begin{aligned}
\hat{\mathbf{e}}_i \cdot \hat{\mathbf{e}}_j &= \delta_{ij} \\
\hat{\mathbf{e}}_i \times \hat{\mathbf{e}}_j &= \varepsilon_{ijk}\hat{\mathbf{e}}_k \\
\mathbf{A} \times \mathbf{B} &= \varepsilon_{ijk}a_j b_k \hat{\mathbf{e}}_k \\
\mathbf{A} \cdot \mathbf{B} &= a_i b_i \\
\nabla(\psi) &= \partial_i \psi \\
\nabla \cdot \mathbf{A} &= \partial_i a_i \\
\nabla \times \mathbf{A} &= \varepsilon_{ijk}\partial_j a_k
\end{aligned}$$

A.4 Vector Identities

$$\mathbf{A} + \mathbf{B} = \mathbf{B} + \mathbf{A} \tag{119}$$

Proof.

$$\begin{aligned}
\mathbf{A} + \mathbf{B} &= a_i + b_i \\
&= b_i + a_i \\
&= \mathbf{B} + \mathbf{A}\square
\end{aligned}$$

$$\mathbf{A} \cdot \mathbf{A}^* = |\mathbf{A}|^2 \tag{120}$$

Proof.

$$\begin{aligned}
\mathbf{A} \cdot \mathbf{A}^* &= a_i a_i^* \\
&= |a_i|^2 \\
&= |\mathbf{A}|^2\square
\end{aligned}$$

$$\mathbf{A} \cdot \mathbf{B} = \mathbf{B} \cdot \mathbf{A} \tag{121}$$

$$\mathbf{A} \times \mathbf{B} = -\mathbf{B} \times \mathbf{A} \tag{122}$$

Proof.

$$\begin{aligned}\mathbf{A}\times\mathbf{B} &= \varepsilon_{ijk}a_i b_j \hat{\mathbf{e}}_k \\ &= -\varepsilon_{jik}b_j a_i \hat{\mathbf{e}}_k \\ &= -\mathbf{B}\times\mathbf{A}\ \square\end{aligned}$$

$$(\mathbf{A}+\mathbf{B})\cdot\mathbf{C} = \mathbf{A}\cdot\mathbf{C}+\mathbf{B}\cdot\mathbf{C} \tag{123}$$

$$(\mathbf{A}+\mathbf{B})\times\mathbf{C} = \mathbf{A}\times\mathbf{C}+\mathbf{B}\times\mathbf{C} \tag{124}$$

$$\mathbf{A}\cdot(\mathbf{B}\times\mathbf{C}) = \mathbf{B}\cdot(\mathbf{C}\times\mathbf{A}) = \mathbf{C}\cdot(\mathbf{A}\times\mathbf{B}) \tag{125}$$

Proof.

$$\begin{aligned}\mathbf{A}\cdot(\mathbf{B}\times\mathbf{C}) &= (a_i\hat{\mathbf{e}}_i)\cdot\varepsilon_{lmn}b_l c_m\hat{\mathbf{e}}_n \\ &= \varepsilon_{lmn}a_i b_l c_m(\hat{\mathbf{e}}_i\cdot\hat{\mathbf{e}}_n) \\ &= \varepsilon_{lmn}a_i b_l c_m\delta_{in} \\ &= \varepsilon_{nlm}a_n b_l c_m \\ &= \varepsilon_{mnl}b_m c_n a_l \\ &= \mathbf{B}\cdot(\mathbf{C}\times\mathbf{A}) \qquad \square\end{aligned}$$

$$\mathbf{A}\times(\mathbf{B}\times\mathbf{C}) = (\mathbf{C}\cdot\mathbf{A})\mathbf{B}-(\mathbf{B}\cdot\mathbf{A})\mathbf{C} \tag{126}$$

Proof.

$$\begin{aligned}\mathbf{A}\times(\mathbf{B}\times\mathbf{C}) &= a_i\hat{\mathbf{e}}_i\times\varepsilon_{lmn}b_l c_m\hat{\mathbf{e}}_n \\ &= \varepsilon_{lmn}a_i b_l c_m(\hat{\mathbf{e}}_i\times\hat{\mathbf{e}}_n) \\ &= \varepsilon_{lmn}\varepsilon_{ink}a_i b_l c_m\hat{\mathbf{e}}_k \\ &= \varepsilon_{nlm}\varepsilon_{nki}a_i b_l c_m\hat{\mathbf{e}}_k \\ &= (\delta_{lk}\delta_{mi}-\delta_{li}\delta_{mk}a_i b_l c_m\hat{\mathbf{e}}_k) \\ &= c_i a_i b_k\hat{\mathbf{e}}_k - b_i a_i c_k\hat{\mathbf{e}}_k \\ &= (\mathbf{C}\cdot\mathbf{A})\mathbf{B}-(\mathbf{B}\cdot\mathbf{A})\mathbf{C}\ \square\end{aligned}$$

$$\mathbf{A}\times(\mathbf{B}\times\mathbf{C}) = (\mathbf{C}\cdot\mathbf{A})\mathbf{B}-(\mathbf{B}\cdot\mathbf{A})\mathbf{C} \tag{127}$$

Proof.

$$\begin{aligned}
\mathbf{A}\times(\mathbf{B}\times\mathbf{C}) &= a_i\hat{\mathbf{e}}_i\times\varepsilon_{lmn}b_lc_m\hat{\mathbf{e}}_n \\
&= \varepsilon_{lmn}a_ib_lc_m(\hat{\mathbf{e}}_i\times\hat{\mathbf{e}}_n) \\
&= \varepsilon_{lmn}\varepsilon_{ink}a_ib_lc_m\hat{\mathbf{e}}_k) \\
&= \varepsilon_{nlm}\varepsilon_{nki}a_ib_lc_m\hat{\mathbf{e}}_k) \\
&= (\delta_{lk}\delta_{mi}-\delta_{li}\delta_{mk})a_ib_lc_m\hat{\mathbf{e}}_k) \\
&= c_ia_ib_k\hat{\mathbf{e}}_k - b_ia_ic_k\hat{\mathbf{e}}_k \\
&= (\mathbf{C}\cdot\mathbf{A})\mathbf{B}-(\mathbf{B}\cdot\mathbf{A})\mathbf{C} \quad \square
\end{aligned}$$

$$\nabla(\psi+\phi)=\nabla\psi+\nabla\phi \tag{128}$$

Proof.

$$\begin{aligned}
\nabla(\psi+\phi) &= \partial_i(\psi+\phi) \\
&= \partial_i\psi+\partial_i\phi \\
&= \nabla\psi+\nabla\phi\square
\end{aligned}$$

$$\nabla(\psi\phi)=\psi\nabla\phi+\psi\nabla\phi \tag{129}$$

Proof.

$$\begin{aligned}
\nabla(\psi\phi) &= \partial_i(\psi\phi) \\
&\overset{chain\ rule}{=} \psi\partial_i\phi+\psi\partial_i\phi \\
&= \psi\nabla\phi+\phi\nabla\psi\square
\end{aligned}$$

$$\nabla\cdot(\mathbf{A}+\mathbf{B})=\nabla\cdot\mathbf{A}+\nabla\cdot\mathbf{B} \tag{130}$$

$$\nabla\cdot(\psi\mathbf{A})=\psi\nabla\cdot\mathbf{A}+\mathbf{A}\cdot\nabla\psi \tag{131}$$

Proof.

$$\begin{aligned}
\nabla\cdot(\psi\mathbf{A}) &= \partial_i(\psi a_i) \\
&\overset{chain\ rule}{=} \psi\partial_i a_i+a_i\partial_i\psi \\
&= \psi\nabla\mathbf{A}+\mathbf{A}\cdot\nabla\psi\square
\end{aligned}$$

$$\nabla \cdot (\mathbf{A} \times \mathbf{B}) = \mathbf{B}(\nabla \times \mathbf{A}) - \mathbf{A} \cdot (\nabla \times \mathbf{B}) \tag{132}$$

Proof. Check (127). □

(133)

$$\nabla \times (\mathbf{A} + \mathbf{B}) = \nabla \times \mathbf{A} + \nabla \times \mathbf{B} \tag{134}$$

$$\nabla \times (\psi \mathbf{A}) = \psi \nabla \times \mathbf{A} + \mathbf{A} \times \nabla \psi \tag{135}$$

$$\nabla \cdot \nabla \times \mathbf{A} = 0 \tag{136}$$

Proof. For a three-dimensional system:

$$\begin{aligned} \nabla \cdot \nabla \times \mathbf{A} &= \partial_i(\varepsilon_{ijk})\partial_j a_k \\ &\overset{explicit\ sum}{=} \partial_i(\varepsilon_{ijk}\partial_j a_k + \varepsilon_{ikj}\partial_k a_j) \\ &\quad +\partial_j(\varepsilon_{jki}\partial_k a_i + \varepsilon_{jik}\partial_i a_k) \\ &\quad +\partial_k(\varepsilon_{kij}\partial_i a_j + \varepsilon_{kji}\partial_j a_i) \\ &= 0 \end{aligned} \tag{137}$$

□

$$\nabla \times \nabla \psi = 0 \tag{138}$$

$$\nabla \cdot \nabla \psi = \nabla^2 \psi \tag{139}$$

$$\nabla \times (\nabla \times \mathbf{A}) = \nabla(\nabla \cdot \mathbf{A}) - \nabla^2 \mathbf{A} \tag{140}$$

Proof.

$$\begin{aligned} \nabla \times (\nabla \times \mathbf{A}) &= \varepsilon_{ijl}\partial_j(\varepsilon_{lmn}\partial_m a_n) \\ &= \varepsilon_{lij}(\varepsilon_{lmn}\partial_j\partial_m a_n) \\ &= (\delta_{im}\delta_{jn} - \delta_{in}\delta_j m)\partial_j\partial_m a_n \\ &= \partial_m\partial_n a_n - \partial_m\partial_m a_n \\ &= \nabla(\nabla \cdot \mathbf{A}) - \nabla^2 \mathbf{A} \qquad \square \end{aligned}$$

A.5 Dyadic tensors identities

$$\mathbf{A}\cdot\bar{\bar{\mathbf{D}}} = \bar{\bar{\mathbf{D}}}^T\cdot\mathbf{A} \tag{141}$$

$$\left(\mathbf{A}\times\bar{\bar{\mathbf{D}}}\right)^T = -\left(\bar{\bar{\mathbf{D}}}^T\times\mathbf{A}\right) \tag{142}$$

$$\bar{\bar{\mathbf{D}}}\cdot(\mathbf{A}\times\mathbf{B}) = -(\bar{\bar{\mathbf{D}}}\times\mathbf{B})\cdot\mathbf{A} = (\bar{\bar{\mathbf{D}}}\times\mathbf{A})\cdot\mathbf{B} \tag{143}$$

$$\mathbf{A}\times(\mathbf{B}\times\bar{\bar{\mathbf{D}}}) = \mathbf{B}(\mathbf{A}\cdot\bar{\bar{\mathbf{D}}}) - (\mathbf{A}\cdot\mathbf{B})\bar{\bar{\mathbf{D}}} \tag{144}$$

$$(\mathbf{A}\times\bar{\bar{\mathbf{D}}})\cdot\mathbf{B} = \mathbf{A}\times(\bar{\bar{\mathbf{D}}}\cdot\mathbf{B}) \tag{145}$$

$$(\mathbf{A}\cdot\bar{\bar{\mathbf{D}}})\times\mathbf{B} = \mathbf{A}\cdot(\bar{\bar{\mathbf{D}}}\times\mathbf{B}) \tag{146}$$

$$(\mathbf{A}\times\bar{\bar{\mathbf{D}}})\times\mathbf{B} = \mathbf{A}\times(\bar{\bar{\mathbf{D}}}\times\mathbf{B}) \tag{147}$$

$$\nabla\cdot(\psi\bar{\bar{\mathbf{D}}}) = (\nabla\psi)\cdot\bar{\bar{\mathbf{D}}} + \psi\nabla\cdot\bar{\bar{\mathbf{D}}} \tag{148}$$

$$\nabla\times(\psi\bar{\bar{\mathbf{D}}}) = (\nabla\psi)\times\bar{\bar{\mathbf{D}}} + \psi\nabla\times\bar{\bar{\mathbf{D}}} \tag{149}$$

$$\nabla\cdot(\mathbf{A}\times\bar{\bar{\mathbf{D}}}) = (\nabla\times\mathbf{A})\cdot\bar{\bar{\mathbf{D}}} - \mathbf{A}\cdot\nabla\times\bar{\bar{\mathbf{D}}} \tag{150}$$

$$\nabla\times(\nabla\times\bar{\bar{\mathbf{D}}}) = \nabla(\nabla\cdot\bar{\bar{\mathbf{D}}}) - \nabla^2\bar{\bar{\mathbf{D}}} \tag{151}$$

A.5.1 Unit dyadic tensor properties

$$\bar{\bar{\mathbf{I}}} = \bar{\bar{\mathbf{I}}}^T \tag{152}$$

$$\mathbf{A} \cdot \bar{\bar{\mathbf{I}}} = \mathbf{A} \tag{153}$$

$$\bar{\bar{\mathbf{I}}} \times \mathbf{A} = \mathbf{A} \times \bar{\bar{\mathbf{I}}} \tag{154}$$

$$\nabla \cdot (\psi \bar{\bar{\mathbf{I}}}) = \nabla \psi \tag{155}$$

$$\nabla \cdot (\bar{\bar{\mathbf{I}}} \times \mathbf{A}) = \nabla \times \mathbf{A} \tag{156}$$

$$\nabla \times (\psi \bar{\bar{\mathbf{I}}}) = \nabla \psi \times \bar{\bar{\mathbf{I}}} \tag{157}$$

APPENDIX **B**

Depolarization dyadic examples

Table 5: Depolarization dyadic for some widely used shapes

Shape	Depolarization Dyadic	Figure
Sphere	$\frac{\bar{\bar{\mathbf{I}}}}{3}$	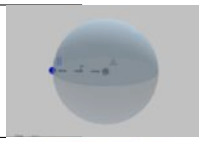
Cube at center	$\frac{\bar{\bar{\mathbf{I}}}}{3}$	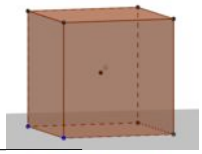
Pillbox	$(1-\frac{h}{2r})\mathbf{e}_z\mathbf{e}_z+\frac{h}{4r}(\mathbf{e}_x\mathbf{e}_x+\mathbf{e}_y\mathbf{e}_y)$	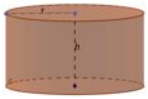
Ellipsoid	$N_x\mathbf{e}_x\mathbf{e}_x+N_y\mathbf{e}_y\mathbf{e}_y+N_z\mathbf{e}_z\mathbf{e}_z$	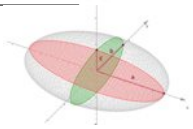

A much more exhaustive list may be founded on (BLADEL, 2007) and (YAGHJIAN, 1980).

APPENDIX C

Parameter extraction algorithm

The samples presented in Chapter 7 had inclusions in a very low volume fraction and since the resin (the host material) is low-loss, a low-loss mixture was expected.

In order to calculate the constitutive parameters of a low-loss material using the waveguide method and the S-parameters measurements a modified version of the classical Nicolson-Ross-Wier (NRW) (NICOLSON; ROSS, 1970) was used. This method was introduced by Adriano Luiz de Paula et al. in (PAULA; BARROSO; REZENDE, 2011).

The final expression for the measured permittivity is a function of only the S_{11} and S_{21} scattering parameters, the cutoff frequency of the waveguide used, the thickness of the sample and the frequency of the illuminating field. The formula, derived on de Paula's paper, is given by:

$$\mu_r = \frac{\lambda_{0g}}{\Lambda} \cdot \frac{1+\Gamma}{1-\Gamma} \tag{158}$$

$$\epsilon_r = \frac{\lambda_0^2}{\mu_r} \cdot \left(\frac{1}{\Lambda^2} + \frac{1}{\lambda_c}\right) \tag{159}$$

where λ_c is the cutoff frequency of the waveguide (6.4Ghz in the experiments made) and

$$\lambda_{0g} = \frac{\lambda_0}{\sqrt{1-(\frac{\lambda_0}{\lambda_c})^2}} \tag{160}$$

$$\Lambda = \frac{j}{2\pi d} ln(T) \tag{161}$$

$$\tag{162}$$

Where Γ and T are the reflection and transmission coefficients calculated with the S-parameters given.

A much more extensive list of algorithms for parameter extraction may be found on (KUEK, 2006).

APPENDIX D

Experimental setup

In order to measure the S-parameters a VNA Rohde&Swarz ZNA-40 was used. Using its TCP/IP communication, the VNA was connected to a computer running a Python script to automatically calculate the effective permittivity once the S_{11} and S_{21} were measured.

For all samples the measurements were made in the X-band in a rectangular waveguide mounted as shown in Figure (19).

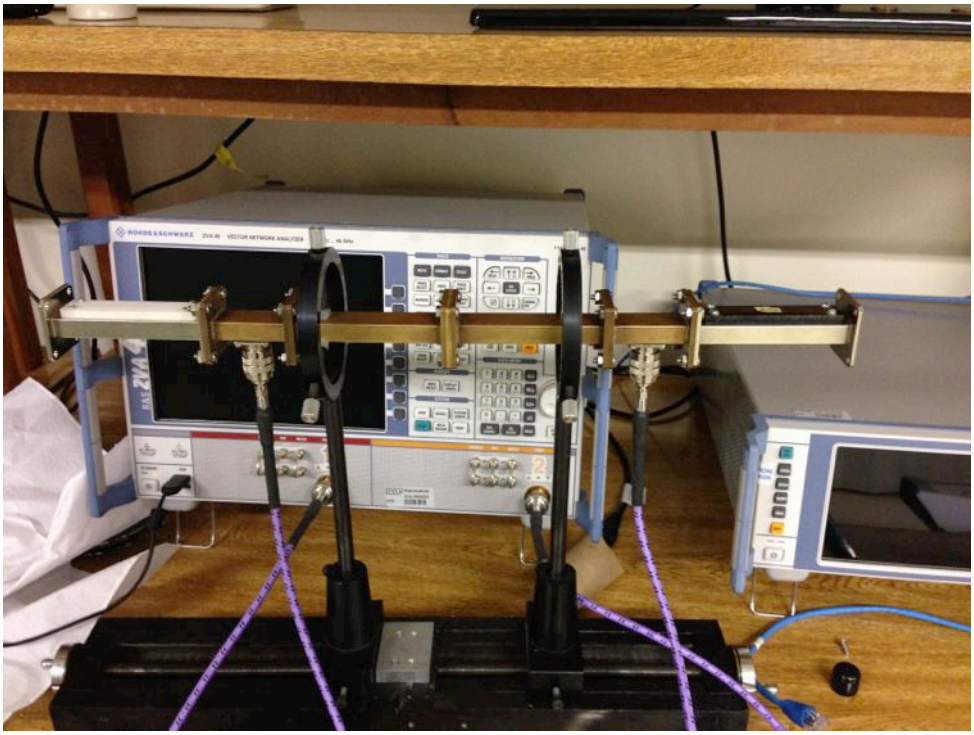

Figure 19: Experimental setup with rectangular waveguides, a sample holder (waveguide flange), attenuators and the VNA

Figure (20) gives the general shape and inner dimensions of the waveguide. Using equation (163) one can calculate the cutoff frequency of this guide for TE10 waves.

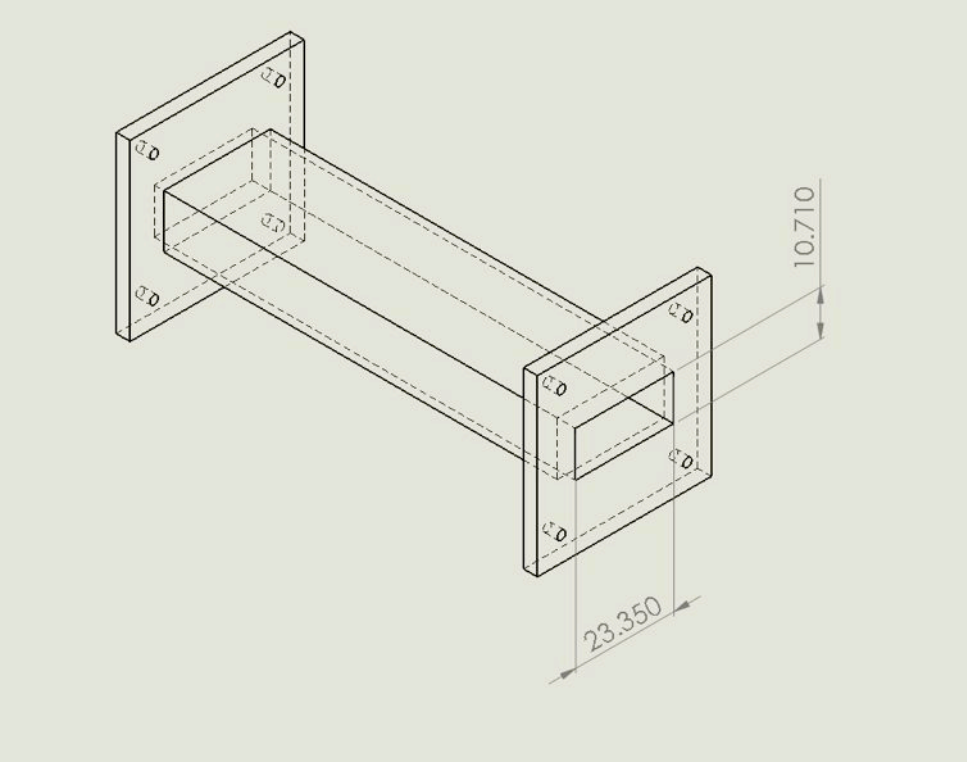

Figure 20: Typical rectangular waveguide used for the measurements

$$f_c = \frac{c}{2a} \tag{163}$$

where 'a' is the larger internal dimension of the guide in meters and c is the speed of light.

The calculated value of 6.42GHz matches perfectly the measured cutoff frequency.

One may note that in both left and right terminations of the waveguide the ends have attenuators with ends opened. The goal of having this setup is to minimize internal reflections, avoiding the waveguide behaving like a cavity resonator.

D.1 VNA calibration procedure

Before a series of measurements the VNA should be calibrated appropriately. The most appropriate calibration for the measurements with waveguides is the thru-reflect-line(TRL) calibration procedure. For the VNA used, the best algorithm was the *NIST optimized TRL* that may be found as one of the calibration options. The TRL calibration is done in three stages:

- ❏ Thru: all the waveguides are connected without any sample holder or separator
- ❏ Line: a $\lambda/4$ flange is used to separate the two waveguides, as shown in Figure (21). In this case we chose 10GHz as central frequency and the flage has to have 3.5mm length.

❑ Reflect: both waveguides are covered by a mirror (a piece of metal)

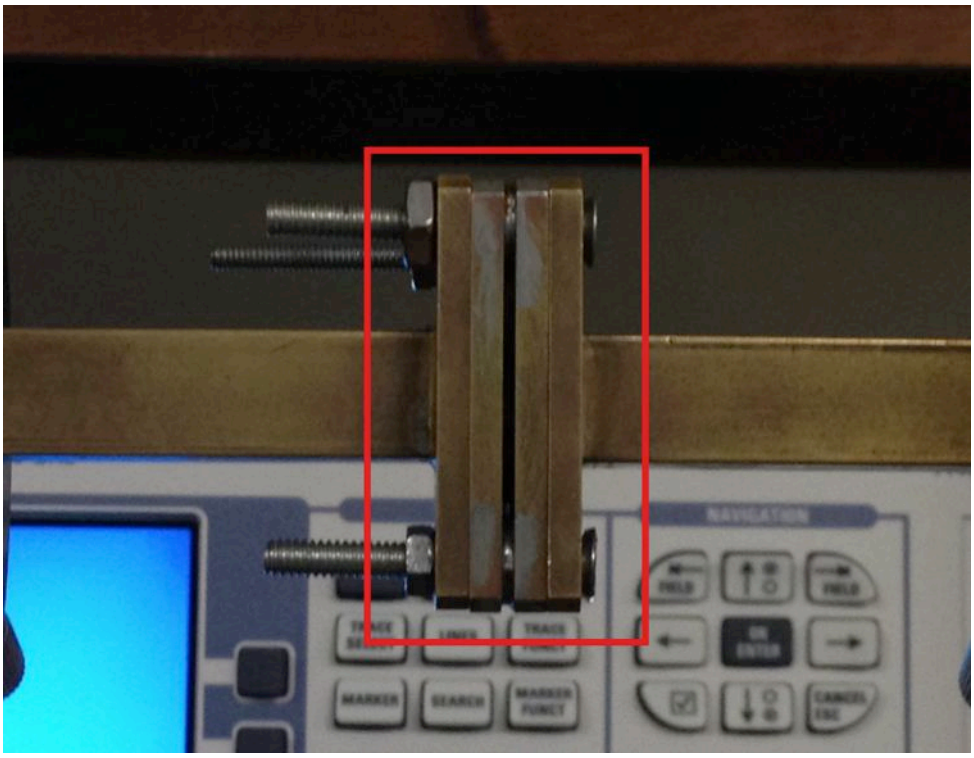

Figure 21: Example of quarter-wave flange used for calibration Line procedure

D.2 Sample holders

The sample holders consisted of metal flanges of several thicknesses to match the thickness of the measured sample. Thicknesses differences between the sample and the holder must be compensated in the VNA by software, introducing the new air path introduced by the thicknesses differences.

Besides the thickness difference, the holders were also different by how the sample would be put on it: for some holders (Figure (22)) the sampled would be cut and snapped in and for others (Figure (23)) the sample would be cured inside of it and the sample would be then permanently attached to it.

Both types of holders have drawbacks: the geometrical differences between the sample and the holder of the first kind would create air gaps that needs to be compensated (KUEK, 2006), (NOTE, 2006). For the second type of holders, during the curing process of the resin, air bubbles couldn't get out of the sample and would be present on it after the curing was done.

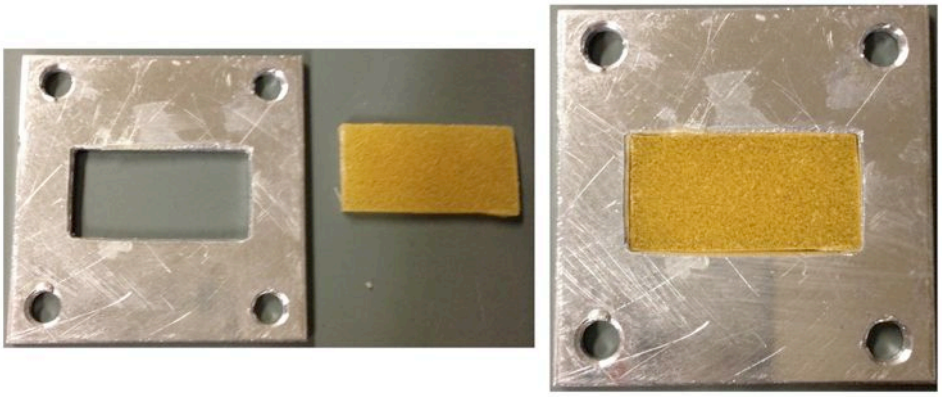

Figure 22: Holder were the sample must be snapped into it before the measurement. Air gaps due to geometric differences must be compensated on the post-processing of the S-parameters measured.

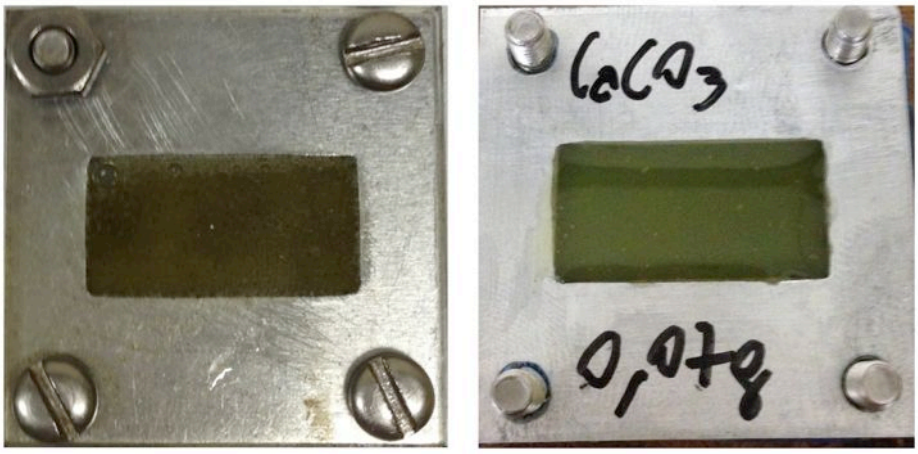

Figure 23: Holders were the resin was cured on it. The sample was attached to the holders permanently. On the first picture the holder is sandwiched by two plastic flanges in order to make the sample as flat as possible. Second picture shows a holder before snapping the top flange.